



Asymptotic scalings of fluid, incompressible “electron-only” reconnection instabilities: Electron-magnetohydrodynamics tearing modes

H. Betar, D. Del Sarto

► To cite this version:

H. Betar, D. Del Sarto. Asymptotic scalings of fluid, incompressible “electron-only” reconnection instabilities: Electron-magnetohydrodynamics tearing modes. *Physics of Plasmas*, 2023, 30 (7), 10.1063/5.0155211 . hal-04561938

HAL Id: hal-04561938

<https://hal.science/hal-04561938>

Submitted on 28 Apr 2024

HAL is a multi-disciplinary open access archive for the deposit and dissemination of scientific research documents, whether they are published or not. The documents may come from teaching and research institutions in France or abroad, or from public or private research centers.

L'archive ouverte pluridisciplinaire **HAL**, est destinée au dépôt et à la diffusion de documents scientifiques de niveau recherche, publiés ou non, émanant des établissements d'enseignement et de recherche français ou étrangers, des laboratoires publics ou privés.

Asymptotic scalings of fluid, incompressible "electron-only" reconnection instabilities: electron-magnetohydrodynamics tearing modes

H. Betar^{1, a)} and D. Del Sarto^{2, b)}

¹⁾*Laboratoire M2P2, UMR 7340 CNRS – Université Aix-Marseille, F-13451 Marseille, France*

²⁾*Institut Jean Lamour, UMR 7198 CNRS – Université de Lorraine, F-54000 Nancy, France*

(Dated: 3 July 2023)

We perform a numerical study of the scaling laws of tearing modes in different parameter regimes of incompressible fluid electron magnetohydrodynamics (EMHD), both in the small and large wavelength limits, as well as for the fastest growing mode that can be destabilized in a large aspect ratio current sheet. We discuss the relevance of these results, also for the interpretation of the "electron-only reconnection regime", recently identified in spacecraft measures and in numerical simulations of solar wind turbulence. We restrict here to a single parameter study, in which we selectively consider only one non-ideal effect among electron inertia, perpendicular resistivity and perpendicular electron viscosity, and we also consider the cases in which a proportionality exists between the parallel and the perpendicular dissipative coefficients. While some known theoretical results are thus confirmed, in other regimes and/or wavelength limits, corrections are proposed with respect to some theoretical estimates already available in literature. In other cases, the scalings are provided for the first time. All numerical results are justified in terms of heuristic arguments based on the measurement of the scaling laws of some new microscopic scales associated to the gradients of the eigenfunctions. The alternative scalings we have found are consistent with this interpretation.

^{a)}Electronic mail: homam.betar@univ-amu.fr

^{b)}Electronic mail: daniele.del-sarto@univ-lorraine.fr

I. INTRODUCTION

In this work we revise and complement with some new results the normal mode problem for tearing-type modes¹ in incompressible, slab geometry electron-magnetohydrodynamics (EMHD). We consider the case in which a finite electron inertia, electron-electron viscosity and electron-ion viscosity (i.e., resistivity) separately allow magnetic reconnection. In some regimes this problem has been already addressed in literature by analytically solving the boundary layer equations^{2–10}, or by means of numerical integration^{6,10–12} in some parameter range. The asymptotic scalings so obtained were not always in agreement. Here we address the problem by relying on a version of the numerical solver presented in Ref. 13, purposidly adapted to the set of EMHD equations, and on elements of the heuristic-type analysis recently discussed in Ref.14. In this way we perform a systematic numerical scan of the growth rate and of the current layer width in the different wave-length limits respectively corresponding to the so-called small- Δ' , large- Δ' , and fastest growing mode regimes. We complement these results with the scalings of some characteristic scales lengths associated to the gradients of the eigenfunctions.

Most of the theoretical predictions already available in literature for the single parameter dependence of EMHD tearing modes are confirmed, although with a few exceptions: a correction of the asymptotic EMHD scalings in the long wave-length (i.e., large- Δ') limit is proposed with respect to the only previously available theoretical estimates obtained in all the collisionless⁶, resistive⁸ and viscous¹⁰ regimes. The new scalings obtained in the collisionless regime allow us to interpret and understand in terms of heuristic arguments the discrepancies between the numerical results and theoretical estimates of the scalings of the fastest growing mode, which were already noted in Ref. 11: the new theoretical predictions based on the corrected scaling in the large- Δ' limit allow us to analytically recover the numerical results therein. In all wave-length limits and in all regimes which we have considered, the results which were already available in literature are also complemented with the identification of the scalings of other microscopic scales related to the spatial gradients of the eigenfunctions, which have been only recently identified and/or characterized in Ref. 14. The scalings of the fastest growing mode in a large aspect ratio, static current sheet are also systematically discussed—in most regimes for the first time—and some threshold conditions, possibly relevant for the application of these scalings to turbulent reconnection, are presented. All these results are summarized in Table I.

The agreement of previous theoretical estimates with the numerical results we have obtained for the short wave-length limit of tearing modes in all resistive regimes is instead shown for some examples in Table II.

We also discuss the relevance of incompressible EMHD tearing modes to the more recent notion of "electron-only" reconnection, which has been recently identified and discussed in connection especially with the turbulent solar wind plasma (see, e.g., 15–23 just to cite a few examples of an increasingly large literature), and of which, we argue, the incompressible EMHD represents the fluid, cold, non-relativistic limit.

The article has the following structure:

In Sec. II we introduce the equations and we recall the key features and limitations of the incompressible EMHD model.

In Sec. III we compare the EMHD regime to the identifying features of the so-called "electron-only reconnection" regime: we recall and discuss the main points which possibly justify the applicability of the tearing mode theory to magnetic reconnection in turbulence, and we discuss why EMHD can well represent the incompressible, cold fluid limit of the electron-only reconnection regime, which has been identified in spacecraft measures and kinetic simulations of solar wind turbulence.

In Sec. IV we introduce the key elements of the linear problem: the linearized equations; the equilibrium profiles we are going to consider; the operational definition of the characteristic lengths associated to the spatial gradients of the eigenfunctions; and the hypotheses with which the latter can be used in heuristic-type estimates of the tearing mode scalings.

In Sec. V we discuss the relative orderings of the non-ideal EMHD parameters in some cases of potential physical interest. We then discuss in this light the relevance and limitations of the single parameter study we perform.

In Sec. VI we present and discuss the numerical results of a single parameter study of the scalings of EMHD tearing modes in different regimes. In comparing our results to those of previous theoretical and numerical studies, we provide heuristic consistency arguments for the scaling we find.

Conclusions follow in Sec. VII.

II. THE EMHD MODEL AND ITS INCOMPRESSIBLE LIMIT

Incompressible, barotropic EMHD is a fluid model for the description of a non-relativistic magnetized plasma at microscopic and fast scales, where the dynamics is dominated by electrons and ions constitute a uniform neutralizing background, which is assumed not to have the time to evolve. In presence of a guide field of uniform amplitude B_0 , the normal modes named “whistler waves” or “helicons” (name initially given to whistler waves in solids, and which has been later used to indicate whistler waves propagating in a bounded domain –see, e.g. Ref. 24) define the characteristic frequency and wave-length of EMHD. Their dispersion relation in the collisionless, incompressible limit reads

$$\omega_w = \Omega_e d_e^2 \frac{k_{||} k}{1 + k^2 d_e^2}. \quad (1)$$

Here d_e is the electron skin depth, related to the ion skin depth by $d_i^2 = m_i d_e^2 / (Z^{1/2} m_e) = c^2 \omega_{pe}^2 m_i / (Z^{1/2} m_e)$, where Z is the ion charge, c the speed of light, ω_{pe} the electron plasma frequency and m_α the mass of the α species, with $\alpha = e, i$ for electrons and ions, respectively; $\Omega_e = eB_0 / (m_e c) = m_i \Omega_i / (Z m_e)$ is the electron cyclotron frequency (Ω_i is that of ions). The label $||$ refers to the component of the wave-vector \mathbf{k} that is parallel to the direction of the guide field.

A. EMHD model equations at non-relativistic fluid velocities

We restrict to non-relativistic fluid velocities and we neglect the ion dynamics while supposing a polytropic closure. By relaxing for the moment the incompressibility assumption, the equations for the density n_e and for the fluid velocity \mathbf{u}_e read

$$\frac{\partial n_e}{\partial t} + \nabla \cdot (n_e \mathbf{u}_e) = 0, \quad (2)$$

$$\left(\frac{\partial \mathbf{u}_e}{\partial t} + \mathbf{u}_e \cdot \nabla \mathbf{u}_e \right) = -\frac{e}{m_e} \left(\mathbf{E} + \frac{\mathbf{u}_e}{c} \times \mathbf{B} \right) - \frac{\nabla P_e}{m_e n_e} + \mu_e \nabla^2 \mathbf{u}_e + \frac{e\eta}{m_e} \mathbf{J}, \quad (3)$$

where we have kept account both of a finite electron-electron collision rate ν_{ee} , which gives rise to the electron viscosity μ_e , and of a finite electron-ion collision rate ν_{ei} , which leads to a resistivity η .

These equations must be coupled to a closure condition on the pressure P_e , which we assume to be of the polytropic kind

$$\frac{\partial}{\partial t} (P_e n_e^{-\Gamma}) + \mathbf{u}_e \cdot \nabla (P_e n_e^{-\Gamma}) = 0, \quad (4)$$

and to Faraday's equation, which, thanks to the null contribution of the ion motion to the current density, reads

$$\nabla \times \mathbf{B} = \frac{1}{c} \frac{\partial \mathbf{E}}{\partial t} + \frac{4\pi}{c} \mathbf{J} = \frac{1}{c} \frac{\partial \mathbf{E}}{\partial t} - \frac{4\pi e}{c} n_e \mathbf{u}_e. \quad (5)$$

It must be emphasized that Eq.(4) is here assumed as a closure condition heuristically compatible with the phenomenon we want to consider, and not as a general closure appropriate for the EMHD range of validity, in which an anisotropic pressure tensor Π_e is instead likely to be met²⁵, especially when the collision rate is small with respect to the cyclotron frequencies and the characteristic scale of the (inverse of the) spatial gradients of the velocity is of the order of $|\mathbf{u}_e|/\Omega_e$.

Also note that continuity Eq.(2) coincides by construction with the charge density equation, when ions are at rest: retaining electron density fluctuations with respect to the equilibrium value n_0 prevents us to neglect the displacement current $(1/c)\partial \mathbf{E}/\partial t$ in Faraday's equation (5), since taking the divergence of the latter and combining it with Gauss law, one trivially re-obtains Eq.(2). Intuitively speaking, this happens because both a charge separation and a displacement current are induced when $n_e - n_0 \neq 0$, since the ion density maintains its initial, uniform value n_0 . This means that the proportionality between \mathbf{u}_e and $\nabla \times \mathbf{B}$ in EMHD is only valid in the incompressible limit, which is justified at non-relativistic phase-velocities, whereas allowing for an electron fluid compressibility corresponds here to a kind of relativistic correction.

While a relativistic, compressible EMHD has been considered to model the current filamentation instability in both the cold collisionless^{26–30} and collisional³¹ limit, to model the generation of magnetic vortices³², and to model magnetic reconnection and “annihilation” processes^{33–36} in the context of laser-plasma interactions, different levels of approximation have been considered for compressible EMHD with a non-relativistic fluid velocity: density fluctuations have been included to study tearing-type modes^{37–40} as first order perturbative corrections proportional to the expansion parameter $(\Omega_e/\omega_{pe})^2 \ll 1$, which appears in the incompressible EMHD equations via the substitution $d_e^2 \rightarrow d_e^2 + (\Omega_e/\omega_{pe})^2$; non-barotropic closures in presence of a guide field have been considered to study magneto-genesis problems induced by a Biermann battery-type effect⁴¹ arising as a consequence of a localized electron heating in 2D-EMHD⁴², to study the collision-

less instability of shock-waves associated to nonlinear magneto-acoustic modes, whose wave-front can be considered as essentially steady at the whistler frequency range⁴³, to study magnetic reconnection⁴⁴, and to model some kinds of magnetic activity in neutron stars^{45,46}; an adiabatic pressure closure with “finite-Larmor-radius-like” corrections in a strong magnetic field⁴⁷ and with a full pressure tensor dynamics combined with the hypothesis of a null heat-flux divergence^{48,49} have been considered as alternative closure conditions to Eq.(4), in order to study the eigenmode problem of tearing modes in warm, collisionless, compressible EMHD; a model including the full pressure tensor dynamics has been used for the linear Weibel instability in the “hydrodynamic limit”⁵⁰, and for both the Weibel and current filamentation instabilities in a warm plasma, while assuming a null heat flux gradient^{51,52}.

Part of the interest in the EMHD modelling, which has attracted such a broad attention in literature since the early 1980s, is related to its mathematical properties, and in particular to the conservations that are implied in its collision-less, barotropic regimes, both in the non-relativistic and relativistic limits. Limiting our attention to the case of non-relativistic fluid velocities, taking the rotational of Eq.(3) for $\mu_e = \eta = 0$ and combining it with the other equations above while writing

$$\mathbf{E} = -\nabla\phi - \frac{1}{c} \frac{\partial \mathbf{A}}{\partial t}, \quad (6)$$

where \mathbf{A} is the electromagnetic vector potential such that $\mathbf{B} = \nabla \times \mathbf{A}$, leads us to the conservation equation

$$\frac{\partial}{\partial t}(\nabla \times \mathbf{P}_e) = \nabla \times [\mathbf{u}_e \times (\nabla \times \mathbf{P}_e)]. \quad (7)$$

Here $\mathbf{P}_e \equiv (m_e \mathbf{u}_e - e\mathbf{A}/c)$ is the electron canonical momentum associated to the fluid flow. The vector under time derivative is the fluid counterpart of the “*generalized (electron) vorticity*” introduced by Dirac⁵³,

$$\Omega_e \equiv \nabla \times \left(\mathbf{u}_e - \frac{e\mathbf{A}}{m_e c} \right) = \boldsymbol{\omega}_e - \frac{e\mathbf{B}}{m_e c}, \quad (8)$$

whose Lagrangian conservation is stated by (7). Using indeed a well known vector identity and Eq.(2), Eq.(7) can be identified with the null Lie derivative of Ω_e/n_e ,

$$\frac{\partial}{\partial t} \left(\frac{\Omega_e}{n_e} \right) + \mathbf{u}_e \cdot \nabla \left(\frac{\Omega_e}{n_e} \right) - \left(\frac{\Omega_e}{n_e} \right) \cdot \nabla \mathbf{u}_e = 0, \quad (9)$$

which states the invariance of the tensor density Ω_e/n_e with respect to the drag of the velocity field \mathbf{u}_e (see, e.g., Ref.54). This corresponds to the topological conservation of the field lines of Ω_e/n_e

during the plasma evolution, which, in the incompressible and “mass-less electron” limit where $\Omega_e/n_e \rightarrow m_e c \mathbf{B}/(en_0)$, implies the well known Alfvén theorem⁵⁵ (conservation of the magnetic flux), Woltjer theorem⁵⁶ (conservation of linking number of flux tubes) and Newcomb connection theorem⁵⁷ (co-variance of the magnetic line equation during the evolution of the plasma flow) —see Ref. 40. Magnetic reconnection can take place when such conservations are broken, which can happen when at least one among d_e , η or μ_e is non-zero.

B. Incompressible EMHD and slab-geometry limit

Incompressible EMHD holds when $|n - n_0| \ll n_0$. Formally speaking, this limit applies to spatial scales $L \lesssim d_i$ and to frequencies $\Omega_i \lesssim \omega \lesssim \Omega_e \ll \omega_{pe}$. In this range, the system of Eqs.(2-5) reduces to a single equation (the equation of the generalized vorticity) for the magnetic field components, since the displacement current can be neglected in Eq.(5) so that

$$\mathbf{u}_e = -d_e^2 \Omega_e \nabla \times (\mathbf{B}/B_0). \quad (10)$$

After normalizing lengths to a reference length L_0 , which we will later assume to be the equilibrium magnetic shear length a , and times to the time scale $\tau_w \equiv L_0^2/(\Omega_e d_e^2)$, the equation of the generalized vorticity in presence of collisions reads

$$\begin{aligned} \frac{\partial}{\partial t} (\mathbf{B} - \tilde{d}_e^2 \nabla^2 \mathbf{B}) = \nabla \times [(\nabla \times \mathbf{B}) \times (\mathbf{B} - \tilde{d}_e^2 \nabla^2 \mathbf{B})] \\ + \nabla^2 (\mathbf{R} \mathbf{B} - V \nabla^2 \mathbf{B}). \end{aligned} \quad (11)$$

Here $\tilde{d}_e = d_e/L_0$ and we have introduced the resistive diffusivity R and the viscous hyperdiffusivity V defined as the ratio between the “whistler time” τ_w and, respectively, the “resistive time” τ_η and the “viscous time” τ_μ , according to:

$$R \equiv \tau_w \frac{\eta c^2}{4\pi L_0^2} = \frac{\tau_w}{\tau_\eta}, \quad V \equiv \tau_w \frac{\mu_e d_e^2}{L_0^4} = \frac{\tau_w}{\tau_\mu}. \quad (12)$$

Notice that, for simplicity, we have here assumed that η and μ_e , and therefore R and V , are scalar quantities. Instead, they are more likely to be tensorial quantities (see below).

Also, for simplicity of notation, from now on we will drop the “ \sim ” symbol in the writing of

186 \tilde{d}_e , leaving as implicit the fact that it is normalized to L_0 .

187 It is not of particular interest to consider here the role of the further expansion parameter
 188 $\Omega_e/\omega_{pe} \lesssim 1$ of the semi-compressional model of Ref. 37, previously mentioned, since for the
 189 purposes of the linear analysis its inclusion just implies a trivial re-scaling of the value of the
 190 (effective) electron skin depth.

191 Chronologically speaking, incompressible EMHD is the first model that has been provided
 192 of the EMHD regime. Although its formalization is typically associated to the review works of
 193 Kingsep, Chukbar and Yan'kov⁵⁸ and of Gordeev, Kingsep, and Rudakov⁵⁹, first applications are
 194 in fact earlier (dating back to the 1965, at least). These encompassed: the propagation of “heli-
 195 con modes” in magnetized laboratory plasmas⁶⁰; the linear study of tearing modes in a plasma
 196 column with a radially sheared, helicoidal magnetic field²; the modelling of electron currents
 197 in fast switches in laboratory⁶¹; and the dynamics of electromagnetic vortices in plasmas and
 198 conductors⁶². The latter subject has been further largely investigated, especially in the context
 199 of laser-plasma interactions^{32,63–70} and in dedicated experiments in helicon devices^{71,72}. Beside
 200 of that, incompressible EMHD has been widely studied for its capability of capturing some es-
 201 sential features of a wide range of phenomena. These include: the propagation and instabil-
 202 ity of linear and nonlinear whistler waves in laboratory magnetized plasmas, which constitutes a
 203 large amount of the experimental studies that have been carried out by Stenzel, Urrutia and co-
 204 workers at the UCLA Basic Plasma Physics Laboratory (see, e.g., Refs.71–77); turbulence^{78–85};
 205 Kelvin-Helmholtz and other shear flow instabilities^{86–88}; and, of course, magnetic reconnection.
 206 The latter, after the seminal work in which Gordeev² applied the tearing mode theory¹ to the
 207 EMHD model, has been studied in different regimes both with linear^{3–7,10–12,89,90} and nonlinear
 208 models^{5,12,39,40,91–95}, and it has been specialized to study the coalescence instability^{96,97}, as well.

209 In particular, in order to study spontaneous reconnection via tearing-type instabilities, it is
 210 convenient to consider the slab geometry limit of Eq.(11): assuming the spatial dependence of \mathbf{B}
 211 to be just on x and y , and the guide field to be along z , we can write $\mathbf{B} = \nabla\psi(x, y, t) \times \mathbf{e}_z + (B_0 +$
 212 $b(x, y, t))\mathbf{e}_z$. Then, the information contained in Eqs.(11) can be split into two scalar equations

$$213 \quad \frac{\partial}{\partial t}(\psi - d_e^2 \nabla^2 \psi) + [b, \psi - d_e^2 \nabla^2 \psi] = R_\perp \nabla^2 \psi - V_\perp \nabla^4 \psi, \quad (13)$$

$$\begin{aligned} \frac{\partial}{\partial t}(b - d_e^2 \nabla^2 b) + [b, b - d_e^2 \nabla^2 b] &= [\nabla^2 \psi, \psi] \\ &+ R_{||} \nabla^2 b - V_{||} \nabla^4 b, \end{aligned} \quad (14)$$

where we have used the customary Poisson-bracket notation for $[f, g] = (\nabla f \times \nabla g) \cdot \mathbf{e}_z$ and we have in principle made distinction between the parallel and perpendicular collision rates ν_{ei} and ν_{ee} , which leads to the further labels $||$ and \perp for the dissipation coefficients R and V . While Eq.(14) is the projection along \mathbf{e}_z of (11), Eq.(13) is more conveniently obtained by making the appropriate substitutions and normalization in the z -component of Eqs.(3).

Direct comparison of Eqs.(13-14) with those of slab geometry, reduced MHD (cf., e.g., Eqs.(1-2) of Ref.13), where τ_w is replaced by the Alfvén time, shows that the perturbation of the guide field, b , plays in EMHD the role of the fluid stream function of the $\mathbf{E} \times \mathbf{B}$ -drift in MHD. The latter drags the magnetic flux function ψ associated, in MHD, to the “poloidal” components \mathbf{B}_\perp . In the collisionless, nonlinear regime, the analogy between EMHD and reduced-MHD reconnection has been addressed in Refs.40 and 91. Eqs.(13-14) display however a slightly more “symmetric” form than their MHD counterpart, both in the argument under time derivative and in the dissipation terms: although R and V can be respectively read as the homologous of the inverse Lundquist number S^{-1} and of the inverse Reynolds number in MHD (cf. definitions (12)), in EMHD they affect both scalar fields ψ and b . In particular, in EMHD the electron-electron viscosity, allows magnetic reconnection in the (x, y) plane by violating the Lagrangian conservation of ψ via V_\perp , as it happens in MHD (cf. Eq.(13)). On the other hand, however, the electron viscosity also affects the evolution of the EMHD fluid vorticity via $V_{||}$. In this sense it plays the role which, in the MHD regime, is played by the ion-ion viscosity on the MHD fluid vorticity (see, e.g. Ref.98).

III. RELEVANCE OF EMHD RECONNECTION AND COMPARISON TO "ELECTRON-ONLY RECONNECTION"

Two main reasons can be recognized, which generally motivate the interest in the study of EMHD tearing modes.

The first one concerns the usefulness that this kind of study can bring in shedding light on the transition from MHD tearing-type reconnection in the Alfvénic regime to the so-called Hall-dominated reconnection. The former is essentially a single-fluid theory, where magnetic reconnection can be interpreted as related to the violation of the frozen-in condition involving ions, alone.

In the Hall-dominated reconnection, instead, two-fluid effects become crucial, multiple layers can be identified in the integration domain, and the magnetic reconnection is made possible only if the frozen-in condition of electrons, too, is relaxed in the innermost layer. Indeed, it has been often suggested (see, e.g., Ref. 4 and 99) that EMHD reconnection may be formally seen as occurring in the limit in which Hall term dominates in Ohm's law, while fluid incompressibility is assumed. More generally, indeed, Eq. (3) is the dominant contribution to generalized Ohm's law including the Hall term, when $m_e/m_i \ll 1$. Therefore, the whole set of Hall-MHD equations converges to Eqs. (3-5) in the limit in which the ion fluid velocity is negligible. On the one hand, however, different models and quantitative characterizations of the "Hall-dominated" reconnection have been proposed^{7,93,95,100–111}, in which whistler dynamics becomes important but which may differ from EMHD. On the other hand, the study of the asymptotic threshold of the current sheet aspect ratio, for which the normalized growth rate becomes of order unity in both collisionless EMHD and reduced MHD¹¹ (i.e., the so-called "*ideal tearing*" critical aspect ratio first devised in the resistive reduced MHD case by Pucci and Velli¹¹²), suggests that the incompressible EMHD-tearing mode scalings should not be trivially recovered as a continuous limit of the scalings of the reduced-MHD case: naming τ_A the Alfvén reference time of reduced-MHD and considering the case of a Harris-pinch magnetic equilibrium profile, in Ref. 11 it was found that the threshold aspect ratio condition for the onset of the fastest tearing mode $\gamma\tau_A \sim O(1)$, which develops when a continuum spectrum of modes can be destabilized¹, occurs in MHD for $(a/L)_{MHD} \sim (d_e/L)^{2/3}$, whereas the tearing mode having $\gamma\tau_w \sim O(1)$ develops in EMHD for $(a/L)_{EMHD} \sim (d_e/L)^{3/8}$. This means that, for a fixed current sheet length L , the critical current sheet thickness of collisionless "ideal" tearing modes is smaller in MHD than in EMHD, since, asymptotically, $a_{MHD}/a_{EMHD} \sim (d_e/L)^{7/24} \ll 1$: in the case of a current sheet shrinking (or stretching) "slowly enough", so to grant the applicability of the linear analysis on a "static" equilibrium profile, this suggests that the current sheet disruption always occur because of EMHD-tearing type modes, if the latter were accessible by just "moving" from ideal MHD to microscopic scales. The fact, instead, that there is enough experimental and numerical evidence of MHD-type reconnection, in which ion dynamics plays a prominent role, motivates a better understanding of the quantitative modelling of the EMHD regime and of its connection to the Hall-dominated MHD reconnection.

The second main reason of interest for EMHD tearing type modes is strongly related, and somewhat complementary, to the point above: it concerns the cases of experimental and numerical evidence of magnetic reconnection in regimes where ion dynamics is negligible. This is related

to the more recent notion of "electron-only" reconnection, with respect to which the term "ion-coupled" reconnection is sometimes used¹⁸ in recent literature, in order to identify the Alfvénic or Hall-dominated magnetic reconnection in which ion dynamics is important, instead. The possibility to start from reconnection at Alfvénic scales and to attain a regime where only the electron dynamics becomes relevant was already pointed out in numerical simulations of Hall-type reconnection^{100,102}, once the current layer thickness shrinks to a sufficiently small scale. In Ref. 100, in particular, it was noted that, while Kelvin-Helmoltz-type modes destabilizing the electron flow are expected to be dominant for a current layer thickness $a < d_e$ (occurrence indeed consistent with the numerical results of Ref. 39, 40, and 91), reconnecting instabilities are expected to dominate for $d_e < a < d_i(\delta B/B_0)$ in a regime where the ion dynamics is negligible —here δB is the characteristic jump of the magnetic field at the sides of the current sheet and B_0 its reference value). In particular, the simulation results of Ref. 100 already suggested that ion dynamics could become negligible in a turbulent regime, once spatial scales sufficiently small were attained (cf. Figs. 1-2 therein). This is indeed the case shown by a more recent set of both experimental data and dedicated numerical studies: in recent years, spacecrafts have provided experimental evidence^{15–17,21,93,113} of reconnection events in the turbulent solar wind, in which the current density is dominantly carried by electrons only. This has been dubbed "*electron-only reconnection*" and has fostered an increasingly high number of dedicated numerical and theoretical studies, in which this regime was shown to be induced by turbulence, even when the latter is initialized at the ion scales —see, e.g., Refs. 18–20, 22, 23, and 114. In Ref. 20 it has been however pointed out that some of the general features of the electron-only reconnection regime can be described by the equations of EMHD. This point of view has been further quantified through the simulation results of Ref. 114. In the latter, enough evidence is provided, from both local analysis of the electron and ion outflows along the reconnecting current sheets (see Fig. 6 therein) and from the quantification of the wavelength scaling of the power spectra, that what can be identified as an electron-only reconnection regime in a 2D spatial dependence geometry, occurs compatibly with the conditions $\mathbf{u}_e \simeq \nabla \times \mathbf{B}$ and $|n_e - n_0| \ll n_0$. These are the conditions which formally lead to the incompressible EMHD equations discussed in Sec. II B.

It is true that kinetic effects can play an important role in the electron-only reconnection discussed in the aforementioned works, as it is suggested for example by the non-negligible electron pressure anisotropy measured close to the electron-only reconnection sites in Ref. 114; and it is true that electron pressure anisotropy is well known to play a dominant effect also in extended

Alfvénic reconnection (see, e.g., Ref. 115). The inclusion of pressure anisotropy in EMHD can be however regarded as an extension of EMHD to compressible "warm" regimes⁴⁸, the same way further non-ideal effects like Finite Larmor Radius corrections or non isotropic pressure closures can be accounted for in tearing-type MHD reconnection.

All this suggests that the incompressible EMHD reconnection, which we discuss in this work, can be indeed considered as the incompressible cold fluid limit of the more recent notion of "electron-only reconnection". This is the point of view which we assume, although a few further comments are due, in this regard, in support of this statement. We develop them below, in Sec. III A

A. EMHD vs. electron-only reconnection

It should be first noted that the hypotheses with which the EMHD model is traditionally introduced are those stated at the beginning of Sec. II B, which rely on the restriction to "small enough" spatial scales and to "short enough" time scales. By then looking at the collective properties of the plasma, this is translated into a restriction on the frequency and on the wavelength of the normal modes propagating in the model: it is this way that one a posteriori verifies that whistler waves (index "w", below) obtained by linearising Eqs. (10-11) satisfy $k_w d_i \gtrsim 1$ and $\Omega_i \lesssim \omega_w \lesssim \Omega_e \ll \omega_{pe}$. However, stated in this form, the conditions of validity of EMHD are "global", in the sense they need to be valid in a spatial and temporal domain much wider than that of the spatial and time oscillations of the whistler wave, as it is implied by the normal mode analysis. Therefore, although these conditions on k and ω can be satisfied in the plasmas generated by fast switches, in helicon devices and in other dedicated experiments (like those of the UCLA Basic Plasma Physics Laboratory quoted above), in which electrons are almost uniformly accelerated over "large" spatial domains, they are unlikely to be verified, when one performs a spectrum analysis of numerical or experimental data in a spatial domain in which the conditions $\mathbf{u}_e \simeq \nabla \times \mathbf{B}$ and $|n_e - n_0| \ll n_0$ are only *locally* satisfied, as it is suggested by the numerical results of turbulent reconnection quoted above.

On the other hand, the tearing mode analysis only requires the spatial Fourier transform to be feasible along the direction of the current sheet extension, and that the latter can be considered as static.

In general, if τ_{cs} is the characteristic evolution time and if L is the characteristic length of the

current sheet, the application of the "simplest", standard tearing mode analysis (upon which we rely, in this work) to the current sheet generated by 2D turbulence, generally requires the following conditions to be satisfied:

i) $\tau_{cs}\gamma \gg 1$, with γ growth rate of the tearing mode, so to be able to perform a linear analysis on a steady current sheet (i.e., so that we can assume $\partial/\partial t = 0$ for equilibrium quantities). This assumption can be heuristically made and then a posteriori verified. As a further simplification, in the following we will then assume the equilibrium configuration to be also static (i.e., the equilibrium b field is independent on space, so that there is not any perpendicular equilibrium flow). This allows us to neglect as a first approximation the role of parallel flow to the current sheet, although we note that this may be an important effect in turbulent reconnection. A parallel flow can indeed make tearing modes compete with Kelvin-Helmholtz-type instabilities, when the velocity gradient is sheared across the current sheet (see, e.g., Refs. 116–119) so to cite some of the earliest works), and a combined tearing-Kelvin Helmholtz type mode can be also encountered, in these cases¹²⁰. Otherwise, a parallel flow $u_{||}$ may have a generally stabilizing role on tearing modes, when the gradient is along the current sheet¹²¹. In general, however, this stabilizing effect can be effectively neglected as long as^{121,122} $\gamma \gtrsim u_{||}/L$. This condition can be argued to be valid whenever a current sheet generated by turbulence develops "plasmoids", i.e., magnetic islands which can be associated to the destabilization of high wavenumber tearing modes, and it can be *a posteriori* verified.

ii) $kL \gg 1$, with k expressing here the tearing mode wave-length which corresponds to the spatial oscillations along the current sheet. In the formal limit $kL \rightarrow \infty$, that is, assuming a large aspect ratio current sheet to be almost "infinitely long" with respect to the mode wavelength, a continuum spectrum of unstable modes may be considered: a standard tearing mode theory may be thus applied disregarding border effects due to the lack of periodicity of the current sheet. This assumption is probably the most delicate to be handled, as no quantitative analysis has been done, so far, to assess this latter approximation. Nevertheless, it is at least implicitly assumed in any existing work addressing the turbulent reconnection in terms of the tearing mode analysis.

iii) The orientation of the background, i.e., "guide" magnetic field is orthogonal to the reconnection plane: although the effect of an in-plane magnetic component has been sometimes included in studies of tearing type reconnection^{123,124}, here we do not consider this possibility. Instead, we assume the presence of a standard guide field. These assumptions are generally compatible with turbulent-induced reconnection, at least in a 2D spatial coordinate dependence. The relative amplitude of the magnetic field in these cases results to depend on the level of magnetic fluctua-

tions and on the plasma β . These factors in principle weigh the transition from an Alfvénic to an Hall-mediated reconnection (see, e.g., Ref. 125).

iv) The curvature of the current sheet is negligible: although corrections related to the current sheet curvature can be included in tearing mode analysis (see, e.g., Refs. 126 and 127 for reduced-MHD reconnection in a tokamak), we neglect them, here. For a local curvature radius of the order of L this assumption gets well along with the $kL \gg 1$ condition. Note that accounting for the current sheet curvature would lead us to consider tearing modes developing on asymmetric magnetic equilibrium profiles. The effect of the latter on the linear and nonlinear evolution of instabilities has been studied in different reconnection regimes (see, e.g., Refs. 128–133 just to cite a few), and also in the EMHD framework¹³⁴.

Hypotheses (i-iv) are quite general and, although they can quantitatively differ in different reconnection regimes, they must in principle hold regardless of the latter. Therefore, if one assumes by "experimental evidence" that in the neighborhood of a current sheet generated by turbulence the conditions $\mathbf{u}_e \simeq \nabla \times \mathbf{B}$ and $|n_e - n_0| \ll n_0$ locally hold for a time interval larger (maybe just by one or two orders of magnitude) than $1/\gamma$, the EMHD tearing theory based on Eqs. (10-11) and on the hypotheses (i)-(iv) above can be in principle applied: in the case in which further effects, such as density fluctuations, or kinetic effects such as a finite temperature or an anisotropic pressure, or the transition to the ion-coupled dynamics should be retained, one could try to look at an extension of the incompressible EMHD model (and/or at bridging it to the Hall-mediated reconnection regime), as mentioned above. In any case, this generally makes the EMHD tearing theory and its possible extensions relevant to these phenomena.

This is why we suggest to identify the incompressible EMHD reconnection as a limit regime of the kinetic electron-only reconnection cases experimentally or numerically observed: in this sense, the study of incompressible EMHD tearing mode may provide a starting point for the theoretical modelling also of electron-only reconnection processes. A similar standpoint is expressed also in Ref. 135: therein, the limit of the nonlinear equations for the so-called inertial-kinetic Alfvén wave model¹³⁶, which allows the modelling of the "inertial whistler-wave turbulence" by means of the collisionless inertial EMHD limit of Eqs. (13-14) of this work, was argued to be relevant to electron-only reconnection.

In support of this point of view it should be finally noted that some agreement between spacecraft reconnection data and EMHD reconnection was already pointed out in previous literature^{93,113}. Moreover, dedicated numerical studies of kinetic reconnection on a single, thin,

current sheet, when both ion and electron dynamics were included in a Vlasov-Maxwell PIC numerical solver, have already shown the occurrence of reconnection in an EMHD-type regime¹⁰⁶. In the work of Ref. 106, in particular, Singh et al. noted that (quoting) "*EMHD-type of flows consisting of magnetized electrons and un-magnetized ions in current sheets could be relevant for a longer time period even on spatial scales comparable to the ion-Larmor radius after the introduction of the magnetic perturbations, which initiate magnetic reconnection. Consequences of such limitations of artificially low ion to electron mass ratio remain largely unexplored.*". This remark seems to be indeed in agreement or at least compatible with the more recent numerical simulations^{18–20,22,23,114} performed with smaller electron-to-ion mass ratios.

IV. EIGENVALUE PROBLEM

Linearization (with labels 0 and 1 indicating respectively equilibrium quantities and perturbations) of Eqs.(13-14) with perturbations $f_1 \sim \exp[iky + \gamma t]$ around an equilibrium with uniform b_0 and $\psi_0 = \psi_0(x)$, leads to an eigenvalue problem that can be cast in the matrix form:

$$[M] \cdot \begin{pmatrix} \psi_1 \\ b_1 \end{pmatrix} = \begin{pmatrix} 0 \\ 0 \end{pmatrix}, \quad (15)$$

$$[M] = \begin{pmatrix} \gamma \mathcal{F} - R_\perp \mathcal{L} + V_\perp \mathcal{H} & -\mathcal{A} \\ -\mathcal{B} & \gamma \mathcal{F} - R_\parallel \mathcal{L} + V_\parallel \mathcal{H} \end{pmatrix}. \quad (16)$$

Here we have introduced the differential operators

$$\mathcal{L} \equiv \frac{\partial^2}{\partial x^2} - k^2, \quad \mathcal{F} \equiv 1 - d_e^2 \mathcal{L}, \quad (17)$$

$$\mathcal{A} \equiv ik(\psi'_0 - d_e^2 \psi_0'''), \quad \mathcal{B} \equiv ik(\psi'_0 \mathcal{L} - \psi_0'''), \quad (18)$$

$$\mathcal{H} \equiv \frac{\partial^4}{\partial x^4} - k^4 - 2k^4 \mathcal{L}. \quad (19)$$

Previous studies have addressed the eigenmode analysis by separately considering the role played by electron inertia^{3,4,6}, resistivity^{2,3} and electron viscosity^{5,10}. Here we revise such results, by providing corrections for some of them, and we complement them with new scalings in the fastest-mode wavelength limit and for some further scale lengths of the eigenmodes.

For this purpose we will discuss numerical results obtained by integrating Eqs.(15) with an

426 adapted version of the solver of Ref.13. We consider magnetic equilibria of the form¹³⁷

$$427 \quad \psi_0 = \frac{B_0 a}{2 \cosh^2(x/a)} \quad \text{in} \quad [-2\pi a, 2\pi a], \quad (20)$$

428 (note that $\psi_0(\pm 2\pi) \lesssim 10^{-5}$ is sufficiently small so that it does not appreciably violates the period-
429 icity in x required by the present version of the solver) or of the form¹³⁸

$$430 \quad \psi_0 = B_0 a \cos\left(\frac{x}{a}\right) \quad \text{in} \quad [-\pi a/2, \pi a/2]. \quad (21)$$

431 From now on, we will assume $L_0 = a$ to be the reference normalization length of the system, while
432 L is the current sheet length, i.e., its “spatial period” in the y direction.

433 In the following we will use “ SD ” and “ LD ” to label, respectively, the small- Δ' (or small wave-
434 length) limit, and the large- Δ' (or large wavelength) limit. The label “ M ” will refer instead to
435 the fastest growing mode that can be destabilized when a continuum spectrum of unstable modes
436 can be excited¹. We recall that, while the asymptotic scalings in the small- and large- Δ' limits do
437 not depend on the magnetic equilibrium profile, those of the fastest growing mode do, since they
438 depend on the power-law dependence that the $\Delta'(ka)$ expression gets in the $ka \ll 1$ limit. In this
439 sense, the equilibria of Eq.(20) and (21) provide two typical examples useful in a domain periodic
440 in x , since they respectively correspond to $\Delta'(ka) \sim (ka)^{-2}$ and $\Delta'(ka) \sim (ka)^{-1}$.

441 We also recall that the notion of “asymptotic limit” means that the normalized non-ideal pa-
442 rameters are much smaller than unity: $d_e^2, R_\perp, R_\parallel, V_\perp, V_\parallel \ll 1$. Numerically speaking, this approxi-
443 mately means, as it has been verified in previous works and in different tearing regimes^{11,13}, that
444 each of these dimensionless parameters must be $\lesssim 0.01$. This is coherent with further numerical
445 results^{12,39} that have shown important discrepancies with respect to theoretical predictions from
446 boundary layer analysis when, e.g., $d_e \sim O(1)$.

447 **A. Some characteristic scale lengths and their role in an heuristic, dimensional-type** 448 **analysis**

Heuristic estimates of the scaling of the growth rate γ and of the reconnecting layer width
(operationally defined¹⁴ as the distance $|x| = \delta$ from the neutral line for which $J''_{z,1}(\delta) = \psi_1^{(iv)}(\delta) =$
0) represent a delicate issue in incompressible EMHD: similarly to what it happens in the warm-

resistive regime of reduced MHD^{13,14}, in the EMHD regimes it is generally not possible to obtain the correct scalings by “trivially” balancing the terms of the equations, differently from what can be done, instead, in the collisionless and resistive MHD regimes¹³⁸. Nevertheless, analogously to what has been shown for reduced-MHD tearing modes¹⁴, it is possible to provide a heuristic interpretation of the asymptotic scalings if we order the spatial derivatives of both the magnetic and “velocity” stream functions, ψ_1 and b_1 , in terms of the usual Δ' parameter¹ and of the D' and Δ'_{v_y} inverse scale lengths recently introduced in Ref. 14:

$$\Delta' \equiv \lim_{\varepsilon \rightarrow 0} \frac{\psi'_{1,(id)}(+\varepsilon) - \psi'_{1,(id)}(-\varepsilon)}{\psi_1(0)} = \frac{2c_1}{c_0}, \quad (22)$$

$$D' \equiv \lim_{\varepsilon \rightarrow 0} \frac{\psi'_1(+\varepsilon) - \psi'_1(-\varepsilon)}{\psi_1(0)}, \quad (23)$$

$$\Delta'_{v_y} \equiv \frac{v_{y,1}(\delta) - v_{y,1}(-\delta)}{v_{y,1}(\delta)} = \frac{2b''_1(\delta)}{b'_1(\delta)}. \quad (24)$$

449 Above, $\psi_{1,(id)}(x)$ corresponds to the “outer” solution of the eigenvalue problem, valid in the
 450 “ideal” region of the domain $|x| \sim L_0$ where, in the boundary layer integration procedure, non-
 451 ideal terms can be neglected (we used the index “(id)” to indicate this). Its limit as $|x| \rightarrow 0$ can be
 452 expressed, like for tearing modes in reduced MHD, as $\lim_{|x| \rightarrow 0} \psi_{1,(id)} \simeq c_0 + c_1|x| + O(x^2)$. Note
 453 that, as discussed in Ref. 14, $D \rightarrow \Delta'$ only in the small- Δ' (i.e., “tearing mode”) wavelength limit,
 454 whereas D' departs from Δ' in the large- Δ' limit.

455 All the numerical results we will discuss next (see Sec. VI) will prove to be coherent with the
 456 heuristic-type interpretation that can be given combining hypotheses (22-29) with $\partial^2/\partial x^2 \gg k^2$
 457 and with the fact that $\lim_{x \rightarrow \delta} \psi'_0 \sim \lim_{x \rightarrow \delta} \psi'''_0 \sim \delta$. Applying these latter orderings, Eqs.(13-14),
 458 once linearized, read

$$\gamma(\psi_1 - d_e^2 \psi''_1) \sim k\delta b_1 + R_\perp \psi''_1 - V_\perp \psi_1^{iv}, \quad (25)$$

$$\gamma(b_1 - d_e^2 b''_1) \sim k\delta \psi''_1 + R_\parallel b''_1 - V_\parallel b_1^{iv}. \quad (26)$$

462 The further hypothesis we will use is the ansatz that the terms of the linearized Eq.(13), all balance
 463 each other, whereas in Eq.(14) the two terms with higher order derivatives are dominant. Note that
 464 the first hypothesis gives, in each regime,

$$\left. \frac{b_1}{\psi_1} \right|_\delta \sim \frac{\gamma}{k\delta}. \quad (27)$$

In particular, we will show all the numerical results to be coherent with the heuristic hypotheses:

$$\frac{\psi'_1}{\psi_1} \sim \frac{1}{l_c}, \quad \frac{\psi_1^{(N)}}{\psi_1} \sim \frac{1}{l_c \delta^{N-1}}, \quad \frac{b_1^{(N)}}{b_1} \sim \frac{1}{\delta^N}, \quad (28)$$

$$l_c \sim (D')^{-1} \quad \text{and} \quad \Delta'_{vy} \sim \delta^{-1}. \quad (29)$$

The quantities δ , Δ' , D' , Δ_{vy} and l_c , can be numerically computed as detailed in Ref. 14. However, a difference should be pointed out with respect to the reduced-MHD case discussed therein, in which the fluid stream function ϕ proportional to the electrostatic field determining the leading term of the in-plane fluid velocity —there corresponding to the $\mathbf{E} \times \mathbf{B}$ -drift speed of the bulk ion plasma— formally replaces the scalar field b of this EMHD regime: in the reduced-MHD case the third of Eqs. (28) is replaced by $\phi''_1 \sim \Delta'_{vy} \phi'_1$, with Δ'_{vy} which can in general differ from δ^{-1} (i.e., the second of Eqs. (29) does not hold in the warm-electron reduced-MHD regime); in MHD, the first of Eqs. (29) is instead found to be replaced by $l_c \sim \max\{(\Delta')^{-1}, (\Delta'_{vy})^{-1}\}$. Nevertheless, a similarity with the warm reduced-MHD case discussed in Ref. 14 must be emphasized: like in that case, the heuristic hypotheses of Eqs. (28-29) do not constitute a closed set of conditions which allow one to determine the asymptotic scalings of the characteristic quantities δ , D' , Δ_{vy} and γ by simple dimensional arguments. In EMHD the numerical evaluation of the scalings of D' turns out to be necessary for this purpose, so as knowledge of the scaling of Δ'_{vy} seems to be necessary in reduced-MHD. We will postpone to some future work a more specific discussion of this issue and a comparison with the reduced-MHD case: below, we will just provide numerical evidence of this interpretation for which, as for the reduced-MHD case, we do not have yet a complete “explanation”, provided in the analytical terms of the boundary layer integration. In this sense, the coherence we provide of the assumptions (28-29) must be read as a kind of “experimental” (i.e., numerical) evidence, hoping it may help to shed light, in the future, about the non-trivial behaviour of the eigenmode solutions in this regime. Then, we address the interested reader to look at Ref. 14 for a more detailed discussion about the failure of the heuristic-type estimates in reduced-MHD tearing and about the usefulness/relevance of having introduced the scale lengths $(D')^{-1}$ and $(\Delta_{vy})^{-1}$, therein.

V. RELEVANCE AND LIMITATIONS OF A SINGLE-PARAMETER STUDY OF EMHD-TEARING MODES

Even for the case of a single non-ideal parameter, the boundary layer integration of EMHD tearing modes results to be more complex, under the technical point of view, than that of reduced MHD. This difficulty is related to the different structure of the equation of the "vorticity" field in EMHD (Eq. (14), here) with respect to the case of reduced MHD, in which the fluid equation expresses the time derivative of a vorticity variable U related to the reduced-MHD fluid stream function φ by $U = \nabla^2 \varphi$. The latter is simpler than the $W = b - d_e^2 \nabla^2 b$ case relating the EMHD vorticity field W to the "fluid" stream function b . Because of this, two matching layers appear in the EMHD boundary layer integration even when a single parameter like d_e or R is considered^{3,6}, differently from the reduced MHD case, in which this occurs only in some regimes where two non-ideal parameters contribute¹³⁹ (see also Ref. 14 for details): in RMHD, indeed, the corrections to the eigenvalues determined by the change of the structure of the equation for φ in the different sub-region of the domain of integration, vanish in the asymptotic limit¹⁴⁰.

It should be also noted that, even in reduced MHD, there are some two-parameter reconnection regimes in which the dispersion relation is known not to display a power law scaling: it is the case where both electron inertia and resistivity contribute with comparable weight, although in reduced-MHD this happens only in a quite limited interval of the parameter space¹³. A preliminary numerical study we have performed, but which is not shown here, indicates that analogous non-power law scalings are measured in EMHD regimes in a broader parameter interval, when more than one non-ideal effect is retained. Moreover, in EMHD this seems to be not limited to the case of combination of d_e and R . Due to the richness of behaviors observed, we will therefore postpone to a future work a more systematic investigation of a multi-parameter dependence of EMHD tearing modes: here we will focus on the single-parameter case only, since, as we are going to show, this alone yields non-trivial results, in some case in disagreement with previous analytical estimates available in literature.

It is then worth spending a few words about the relevance and limitations of a single parameter study to EMHD reconnection regimes of possible experimental interest. To this purpose, it is useful to consider some explicit formula^{141,142} for the quantification of the dimensionless parameters d_e , R_\perp , R_\parallel , V_\perp , and V_\parallel , in terms of some plasma quantities, namely the electron density (n_e) and temperature (T_e), the ion charge (Z), the amplitude of the guide field (B_0), and in terms of the

purely geometrical factor represented by the equilibrium shear length a . This intervenes in the a-dimensioning of the non-ideal parameters (i.e., when we take $L_0 = a$). In the formulae below, $\ln \Lambda$ is the Coulomb logarithm, which generally depends on Z , T_e and n_e , but which typically contributes with a numerical factor of the order of $10 \lesssim \ln \Lambda \lesssim 20$, the temperature is expressed in eV and all other dimensional quantities are written in *cgs* units.

The parallel and perpendicular components of Spitzer's resistivity^{143,144} can be synthetically expressed¹⁴¹ in terms of a characteristic electron collision time

$$\tau_e \simeq \frac{3.44 \times 10^5}{\ln \Lambda} \frac{T_e^{3/2}}{Z n_e} \text{ sec}, \quad (30)$$

as

$$\eta_{\perp} = \mathcal{A}_{\perp}(Z, \Lambda) \frac{m_e}{n_e e^2 \tau_e}, \quad \eta_{\parallel} = \mathcal{A}_{\parallel}(Z, \Lambda) \frac{m_e}{n_e e^2 \tau_e}, \quad (31)$$

where the numerical factors \mathcal{A}_{\parallel} and \mathcal{A}_{\perp} are related to the effective particle scattering in the directions parallel and perpendicular to a magnetic field, and they are such that $0.29 \leq \eta_{\parallel}/\eta_{\perp} \leq 0.51$ for Z formally varying from $Z = +\infty$ to $Z = 1$ (cf. Table I of Ref. 141; see also Ref. 145 for further comments in this regards).

Concerning the electron viscosity and hyperviscosity, we can also rely on Braginskii's estimates of the components of the electron viscous stress tensor¹⁴¹ and generically write

$$\mu_{e,\perp} = \mathcal{B}_{\perp}(Z, \Lambda) \frac{n_e T_e}{\Omega_e^2 \tau_e}, \quad \mu_{e,\parallel} = \mathcal{B}_{\parallel}(Z, \Lambda) n_e T_e \tau_e, \quad (32)$$

where, again, \mathcal{B}_{\perp} and \mathcal{B}_{\parallel} are numerical factors of the order of some decimal unit, and are in general comparable to unity. By substituting $L_0 = a$ in the definition of τ_W we can thus write

$$R_{\perp,\parallel} = \frac{c^2}{4\pi} \frac{\eta_{\perp,\parallel}}{\Omega_e d_e^2} = \frac{\mathcal{A}_{\perp,\parallel}}{\Omega_e \tau_e}, \quad V_{\perp,\parallel} = \frac{\mu_{e,\perp,\parallel}}{\Omega_e a^2}, \quad \tilde{d}_e = \frac{d_e}{a}, \quad (33)$$

where, for the sake of clarity, we have temporarily restored the distinction between d_e , meant as dimensional quantity, and \tilde{d}_e , indicating here its normalized version. Except for numerical factors of order unity, we thus obtain

$$\frac{R_{\perp}}{R_{\parallel}} = \frac{\mathcal{A}_{\perp}}{\mathcal{A}_{\parallel}} \sim O(1), \quad \frac{V_{\perp}}{V_{\parallel}} \sim \frac{1}{(\Omega_e \tau_e)^2}. \quad (34)$$

Since all of Braginskii's estimates used above rely on the hypothesis $\Omega_e \tau_e \gg 1$, it follows that, typically, $V_\perp \ll V_\parallel$ in a strongly magnetized plasma, and that a departure from the previous estimates could be in principle obtained in weakly magnetized plasmas with a sufficiently large electron particle density.

This indicates that a single-parameter dependence is natural for the resistivity, which can be taken to be essentially isotropic, since the difference between R_\perp and R_\parallel in a fully ionized, magnetized plasma with a unique ion species with charge Z is just of a numerical factor comprised^{141,143,144} between 2 (for $Z=1$) and 3 (for $Z \rightarrow \infty$); in particular, the case $R_\parallel = R_\perp = R$ is applicable in the unmagnetized limit. Instead, a strong anisotropy can be expected for the electron viscosity. In particular, the dissipative cases which are most significant for experimental applications, compatible with a Braginskii-type closure valid for $\Omega_e \tau_e \gg 1$, correspond therefore to $R_\perp \sim R_\parallel \sim R$ and $V_\perp \ll V_\parallel$. The appropriateness of Braginskii's-type estimates based on Eqs. (32) is subject to investigation in the framework of transport theory, both for magnetically confined plasma devices and for space plasmas. For example, if Braginskii's estimates for electrons were applicable to the solar wind Hydrogen plasma, based on the values $n_e \simeq 300 \text{ cm}^{-3}$, $B_0 \simeq 10^{-4} \text{ G}$, $T_e \simeq 30 \text{ eV}$ (and thus $\ln \Lambda \simeq 25$) measured at ~ 0.17 solar radii from the Sun surface^{146,147}, one would obtain $\Omega_e \tau_e \sim 10^7$, and thus $R_\perp \sim R_\parallel \sim 10^{-7}$ and $V_\perp/V_\parallel \sim 10^{-14}$, where $V_\parallel \sim 10^{-8}$, if one assumes $a \sim d_i$ in the second of Eqs. (33); there are however indications that a departure from the prediction of Braginskii's model should be expected for the collision time of the solar wind electrons¹⁴⁸. Further constraints should be kept into account for the collisionless case: the applicability of the EMHD model for inertia driven tearing modes for asymptotically small parameters is limited by the small scale separation existing between d_e and d_i , which, for an hydrogen plasma, is only $d_i/d_e \simeq 42$. The requirement $L \lesssim d_i$ combined with the condition $d_e^2 \ll a^2$ imposed by the asymptotic analysis on which the tearing mode theory is grounded, does not leave a wide margin of values available for the shear length a , which should thus be comparable to d_i . For example, for $a \sim d_i$, a normalized value of $d_e \sim 0.023$ —but not a much smaller one— would be meaningful for a hydrogen plasma. At the same time, assuming $a \ll d_i$ to be the normalization length of the system, one sees that likely values of the normalized d_e can be well of the order of $d_e \gtrsim 0.1$, which yields growth rates that depart from the asymptotic tearing-type scaling and are of the order of fractions of $1/\tau_W$ (see Fig. 1 of Ref. 39). Therefore, the range of variability of d_e of practical interest for an asymptotic analysis can be quite limited, especially in astrophysical plasmas, but a wider range of values can be meaningful for laboratory experiments in which heavier ions are

considered. In any case, the collisionless regime has been already addressed by several theoretical works, in the past^{3–6,8–12}.

The actual relevance of a single parameter study should be therefore measured, in a first approximation, with respect to the relative ordering between R , $V_{||}$ and d_e^2 . In this sense, both a purely (isotropic) resistive regime and a purely collisionless regime can be meaningful^{2,3,5,7}, whereas the case $V_{\perp} = V_{||}$ typically is not, although, for analytical simplicity, it is the only one which seems to have been considered, so far, in EMHD^{5,10}. In the following, however, we will not restrict to this rationale: we will proceed instead in a more systematic and formal way –regardless of the experimental applications– by selectively fixing only one among d_e , R_{\perp} and V_{\perp} to be non zero. The choice of retaining, in this study, the perpendicular components of resistivity and viscosity instead of the parallel ones is motivated by the fact that only the former can induce magnetic reconnection in the (x,y) -plane, when $d_e = 0$. Because of this, and in the light of the previous estimates (cf. Eqs.(34)), although some of the 1-parameter regimes we are going to considered below are expected to hold in some specific physical situations, other regimes, which we are going to study, can be regarded as limit cases of theoretical and somewhat "academic" interest. Nevertheless, studying them has a twofold usefulness.

First of all, their study allows an identification of regimes where the reconnection rate gets a clear power law scaling –task which is non trivial, from an analytical point of view, as it appears evident from the fact that the scalings we have numerically obtained and which we discuss below (cf. Table I) do not always confirm the theoretical predictions already available in literature (in the following, we are also going to provide some consistency arguments in support of the scalings we obtain, while comparing them to previous analytical estimates with respect to which they differ). In this sense, a numerical study of these limit cases is of support to the theoretical analysis, too, since it can help in the identification of ranges of parameter towards which the 1-parameter analytical solution should converge. It should be noted, indeed, that in the few cases in which a dispersion relation of EMHD-tearing modes has been obtained via non-trivial boundary layer calculations, specific approximations have been done about the ordering of some characteristic parameters. The final dispersion relation has been obtained only in an implicit and quite complex form (cf., e.g., Eq.(35) of Ref. 6 or Ref. 10), so that, extracting from it self-consistent power law scalings in some limits is not a trivial task and requires further specific heuristic-type assumptions. The latter are not easy to be a posteriori verified, if not numerically.

Then, the second element of usefulness of this one-parameter analysis is that all of the regimes

we consider can provide useful indications for limit cases of a multi-parameter tearing-mode analysis, or for some limits of the possible extensions of the EMHD tearing-mode model (e.g., those that can be obtained by including other kinetic effects, such as the contribution of the full pressure tensor in the EMHD regime). For example, in the case of kinetic electron-only reconnection, both electron inertia and temperature effects are likely to play a fundamental role, together with viscous electron dissipation. These arguments, however, will be addressed and developed in forthcoming works.

VI. ASYMPTOTIC ONE-PARAMETER DEPENDENCE OF EMHD TEARING MODES

Let us now discuss the results of the numerical integration performed in the limit in which, from the mathematical point of view, a single independent parameter is chosen.

The numerical results summarized in Table I provide the asymptotic scalings we have obtained in different limit regimes: in the purely collisionless case dominated by electron inertia, i.e., $d_e \neq 0$ (first column); in the case in which $R_\perp \sim R_\parallel$ and a proportionality relation exists between R_\parallel and R_\perp , which encompasses the "isotropic resistivity" limit $R_\parallel = R_\perp = R$ (second column); in the case —more of mathematical interest— where only R_\perp is different from zero (third column); in the case in which a proportionality relation exists between V_\parallel and V_\perp with $V_\parallel \geq V_\perp$, which encompasses the limit of an "isotropic" electron viscosity $V_\parallel = V_\perp$ (fourth column); in the further case of mathematical interest where V_\perp alone contributes to the reconnection rate (fifth column). Note that the limit $d_e = 0$ is formal and corresponds to the $m_e \rightarrow 0$ limit of Eq.(3) but it does not affect the normalization time we have chosen, since τ_w does not depend on m_e .

All the scalings reported in Table I have been verified numerically. In the collisionless regime (Sec. VI A), and for the smallest values of the non-ideal parameters in the collisional regimes (Sec. VI B), the scalings have been obtained using an arbitrary precision version of the eigensolver, which strongly enhances the numerical convergence of the measured scaling laws (e.g. the scaling of the width of the reconnection layer δ) when the non-ideal parameters become very small. This arbitrary precision algorithm, tested and validated for reduced-MHD in Refs. 13 and 14, was based on the multi-precision toolbox developed by Holoborodko¹⁴⁹. In all other regimes a satisfying convergence has been obtained by using the double precision version of the solver on a non-uniform grid.

TABLE I. : Asymptotic scalings of collisional reduced-MHD tearing modes. The five columns corresponds, in order, to the single-parameter case in which the tearing reconnection rate respectively depends on: d_e (cf. §VI A); on $R = R_\perp = R_\parallel$ (these asymptotic scalings are also applicable to the case $R_\parallel = \mathcal{A}R_\perp$, cf. §VI B); on R_\perp (cf. §VI C); on $V = V_\perp = V_\parallel$ (these asymptotic scalings are also applicable to the case $V_\parallel = \mathcal{B}V_\perp$, cf. §VI D); on V_\perp (cf. §VI E). The lines correspond to the asymptotic scalings of the characteristic scale lengths δ (cf. first line of §IV A), D' and Δ'_{vy} (cf. Eqs. (22)) and of the growth rate γ (cf. Eqs. (25-26)). These are provided first for the large wave-length limit (i.e., large- Δ' , label "LD"), then for the small wave-length limit (i.e., small- Δ' , label "SD") and finally for the fastest growing mode which can be destabilized when a continuum spectrum of tearing modes is allowed (label "M"; cf. Sec. IV before §IV A).

Bottom line refers to the scaling of the critical aspect ratio $(a/L)_{crit}$ discussed in Sec. III.

	inertial	resistive	resistive	viscous	viscous					
	(d_e)	$(R_\perp = R_\parallel = R)$	$(R_\perp, R_\parallel = 0)$	$(V_\perp = V_\parallel = V)$	$(V_\perp, V_\parallel = 0)$					
$\delta_{LD} \sim$	$d_e^{\frac{6}{5}}$	$k^{-\frac{1}{2}} R^{\frac{1}{2}}$	$k^{-\frac{2}{3}} R^{\frac{4}{7}}$	$k^{-\frac{1}{4}} V^{\frac{1}{4}}$	$k^{-\frac{2}{7}} V^{\frac{1}{4}}$					
$(l_c)_{LD} \equiv (D')_{LD}^{-1} \sim$	$d_e^{\frac{4}{5}}$	$k^{-\frac{1}{3}} R^{\frac{1}{3}}$	$R^{\frac{2}{7}}$	$k^{-\frac{1}{4}} V^{\frac{1}{6}}$	$V^{\frac{5}{28}}$					
$(\Delta'_{v_y})_{LD}^{-1} \sim$	$d_e^{\frac{6}{5}}$	$k^{-\frac{1}{2}} R^{\frac{1}{2}}$	$k^{-\frac{2}{3}} R^{\frac{4}{7}}$	$k^{-\frac{1}{4}} V^{\frac{1}{4}}$	$k^{-\frac{2}{7}} V^{\frac{1}{4}}$					
$\gamma_{LD} \sim$	$k d_e^{\frac{2}{5}}$	$k^{\frac{5}{6}} R^{\frac{1}{6}}$	$k^{\frac{2}{3}} R^{\frac{1}{7}}$	$k V^{\frac{1}{12}}$	$k^{\frac{6}{7}} V^{\frac{1}{14}}$					
$\delta_{SD} \sim$	$\Delta' d_e^2$	$k^{-\frac{1}{2}} R^{\frac{1}{2}}$	$k^{-\frac{2}{3}} \Delta'^{\frac{1}{3}} R^{\frac{2}{3}}$	$k^{-\frac{1}{4}} V^{\frac{1}{4}}$	$\Delta'^{\frac{1}{7}} k^{-\frac{2}{7}} V^{\frac{2}{7}}$					
$(l_c)_{SD} \equiv (D')_{SD}^{-1} \sim$	$(\Delta')^{-1}$	$(\Delta')^{-1}$	$(\Delta')^{-1}$	$(\Delta')^{-1}$	$(\Delta')^{-1}$					
$(\Delta'_{v_y})_{SD}^{-1} \sim$	$\Delta' d_e^2$	$k^{-\frac{1}{2}} R^{\frac{1}{2}}$	$k^{-\frac{2}{3}} \Delta'^{\frac{1}{3}} R^{\frac{2}{3}}$	$k^{-\frac{1}{4}} V^{\frac{1}{4}}$	$\Delta'^{\frac{1}{7}} k^{-\frac{2}{7}} V^{\frac{2}{7}}$					
$\gamma_{SD} \sim$	$k(\Delta' d_e)^2$	$\Delta'(kR)^{\frac{1}{2}}$	$(k\Delta')^{\frac{2}{3}} R^{\frac{1}{3}}$	$\Delta' k^{\frac{3}{4}} V^{\frac{1}{4}}$	$\Delta'^{\frac{4}{7}} k^{\frac{6}{7}} V^{\frac{1}{7}}$					
$\Delta'(ka) \xrightarrow[ka \ll 1]{} (ka)^{-p}$	$p = 1$	$p = 2$	$p = 1$	$p = 2$	$p = 1$	$p = 2$	$p = 1$	$p = 2$	$p = 1$	$p = 2$
$\gamma_M \sim$	$d_e^{\frac{6}{5}}$	$d_e^{\frac{4}{5}}$	$R^{\frac{3}{8}}$	$R^{\frac{2}{7}}$	$R^{\frac{1}{3}}$	$R^{\frac{5}{21}}$	$V^{\frac{13}{60}}$	$V^{\frac{17}{108}}$	$V^{\frac{5}{28}}$	$V^{\frac{1}{8}}$
$k_M \sim$	$d_e^{\frac{4}{5}}$	$d_e^{\frac{2}{5}}$	$R^{\frac{1}{4}}$	$R^{\frac{1}{7}}$	$R^{\frac{2}{7}}$	$R^{\frac{1}{7}}$	$V^{\frac{2}{15}}$	$V^{\frac{2}{27}}$	$V^{\frac{1}{8}}$	$V^{\frac{1}{16}}$
$\delta_M \sim$	$d_e^{\frac{6}{5}}$	$d_e^{\frac{6}{5}}$	$R^{\frac{3}{8}}$	$R^{\frac{3}{7}}$	$R^{\frac{8}{21}}$	$R^{\frac{10}{21}}$	$(V^{\frac{13}{60}})$	$(V^{\frac{25}{108}})$	$V^{\frac{13}{56}}$	$V^{\frac{1}{4}}$
$\left(\frac{a}{L}\right)_{crit} \sim$	$(d_e^*)^{\frac{3}{8}}$	$(d_e^*)^{\frac{2}{7}}$	$(R^*)^{\frac{3}{16}}$	$(R^*)^{\frac{1}{7}}$	$(R_\perp^*)^{\frac{1}{6}}$	$(R_\perp^*)^{\frac{5}{42}}$	$(V^*)^{\frac{13}{146}}$	$(V^*)^{\frac{17}{250}}$	$(V_\perp^*)^{\frac{5}{66}}$	$(V_\perp^*)^{\frac{1}{18}}$

The upper half of the Table shows, beside of the scalings of γ and of δ , the scaling of D' and of Δ'_{vy} . The latter two have not been reported in previous works, since these quantities, operationally defined via the second and third of Eqs. (22), respectively, have not been identified in former boundary layer calculations (a partial discussion of their interpretation in the framework of a boundary layer analysis has been done only in Ref. 14, and only for the reduced-MHD case). In particular, the scaling of D' results to be non-trivial in the large- Δ' limit, similarly to what happens for Δ'_{vy} in the reduced-MHD case. In EMHD, instead, we always find that $\Delta'_{vy} \sim \delta^{-1}$. The scalings of δ and those of γ can be compared with the theoretical estimates which have been provided in different regimes, in a number of former works.

TABLE II. : Some values of the growth rates in the small- Δ' limit, which we have obtained numerically (columns of the values γ_{num}), and their ratio with respect to the analytical estimates available from boundary layer calculations (columns of the values γ_{num}/γ_{th}) are shown for different reconnection regimes. We have reported also the reference analytical formulae for γ_{SD} and the corresponding source articles (which appear in the Table as "Refs."). The value $\gamma_{num}/\gamma_{th} \simeq \text{constant}$ is expected as long as the power law scaling holds. Therefore, a slight departure from such constant(s), which in all cases reported below is practically unity, occurs as the values of the normalized non-ideal parameter approach the limits of applicability of the boundary layer theory. This is quite visible in the inertial collisionless regime and in the resistive regime, in which an excellent agreement with the numerical factors of the analytical estimates is measured only for the smaller values of d_e and of R , respectively, which are reported in the upper lines of the Table: a departure from $\gamma_{num}/\gamma_{th} \simeq 1$ appears instead as d_e^2 approaches 10^{-2} and as R approaches 10^{-3} . The range of values of V considered in the viscous case, instead, falls well inside of the asymptotic regime. However, the formula shown for this γ_{SD} regime in the Table differs by a factor 2 with respect to the writing of Eq.(36) of Ref. 10: in the formula below, that factor has been removed from the denominator of Eq.(36) of Ref. 10 in order to grant agreement with the numerical results, which we preliminary assume here as a kind of "experimental evidence" (the convergence of the solver has been tested in all reconnection regimes); in Eq. (112) of Ref. 5, instead, the numerical factors are not reported.

inertial regime: d_e			resistive regime: R			viscous regime: V		
$\gamma_{SD} = \frac{\Gamma^2(\frac{1}{4})}{\Gamma^2(\frac{3}{4})} \frac{k(\Delta' d_e)^2}{4\pi^2}$			$\gamma_{SD} = \frac{\Gamma(\frac{1}{4})}{\Gamma(\frac{3}{4})} \frac{\Delta'(kR)^{\frac{1}{2}}}{2\pi}$			$\gamma_{SD} = \frac{\Gamma(\frac{3}{8})}{\Gamma(\frac{5}{8})} \frac{\Delta'}{\pi} \left(\frac{k^3 V}{8}\right)^{\frac{1}{4}}$		
Refs. ^{3,5-7}			Refs. ^{2,3,7}			Refs. ^{5,10}		
example with $k = 1.78$			example with $k = 1.78$			example with $k = 1.85$		
d_e	γ_{num}	γ_{num}/γ_{th}	R	γ_{num}	γ_{num}/γ_{th}	V	γ_{num}	γ_{num}/γ_{th}
0.02	1.1×10^{-3}	1.	2×10^{-7}	7.5×10^{-4}	1.	5×10^{-9}	9×10^{-3}	0.99
0.04	4.5×10^{-3}	0.97	8×10^{-7}	1.6×10^{-3}	0.99	7×10^{-9}	1×10^{-2}	0.99
0.06	9.5×10^{-3}	0.94	9×10^{-6}	5×10^{-3}	0.98	1×10^{-8}	1.1×10^{-2}	0.99
0.08	1.8×10^{-2}	0.9	6×10^{-4}	4.1×10^{-2}	0.85	5×10^{-8}	1.6×10^{-2}	0.98
0.1	2.8×10^{-2}	0.85	9×10^{-4}	4×10^{-2}	0.81	9×10^{-8}	1.8×10^{-2}	0.98

In general, we have recovered the theoretical predictions of the small- Δ' inertia driven limit^{3,5-7}, of the small- Δ' limit for^{2,3,7} $R_{||} = R_{\perp} = R$, and of the small- Δ' limit for^{5,10} $V_{||} = V_{\perp} = V$. For all these cases, as long as the non-ideal parameters are small enough so to grant applicability of the boundary layer theory, our numerical results are in excellent agreement with the analytical formulae (including possible multiplicative geometrical factors) provided in the aforementioned references, as it shown for some examples in Table II.

Figs.1-10 show the power-law dependence of some quantities with respect to a few of the parameters of interest, in support of the scalings in the table. Therein we have reported the plots of some non-trivial scalings, especially concerning new results or corrections to previous theoretical estimates available in literature.

Concerning the scalings of the growth rate and of the inner layer width, the numerical results we

have obtained in the large- Δ' limits differ, more or less importantly, from the theoretical predictions obtained in all one-parameter regimes previously studied analytically (i.e., the collisionless, the isotropic-resistive and the isotropic-viscous cases): a slight correction in the scalings analytically evaluated in Ref. 6 is found in the inertia-driven case (from $\gamma_{LD} \sim kd_e^{2/3}$ and $\delta_{LD} \sim d_e$ of Ref. 6 to $\gamma_{LD} \sim kd_e^{2/5}$ and $\delta_{LD} \sim d_e^{6/5}$ of this work); the corresponding limit for the purely resistive $R_{||} = R_{\perp} = R$ case agrees with previous estimates⁸ for δ_{LD} , but nor for the growth rate (for which the scaling $\gamma_{LD} \sim k^{3/4}R^{1/4}$ of Ref. 8 must be compared to $\gamma_{LD} \sim k^{5/6}R^{1/6}$ of this work). In the isotropic viscous case $V_{||} = V_{\perp} = V$ the scalings $\gamma \sim k^{7/8}V^{1/8}$ and $\delta \sim k^{-7/32}V^{7/32}$ (the latter only implicitly expressed in Ref. 10 via the relation $V \sim \gamma\delta^4$) obtained in Refs. 5 and 10 are here replaced by the scalings $\gamma_{LD} \sim kV^{1/12}$ and $\delta_{LD} \sim k^{-1/4}V^{1/4}$.

All these results, numerically obtained in the small- and large- Δ' , are unchanged when some proportionality constants \mathcal{A} and \mathcal{B} are fixed between the parallel and perpendicular dissipation coefficients, that is, when $R_{||} = \mathcal{A}R_{\perp}$ and $V_{||} = \mathcal{B}V_{\perp}$. For this, we will show below, as an example, two numerical cases in regimes of possible experimental interest (cf. Sec. V), corresponding to $\mathcal{A} = 0.5$ and to $\mathcal{B} = 10^3$, respectively.

These results will be compared with those obtained in the formal, mathematical limits $R_{\perp} \gg R_{||} \sim 0$ and $V_{\perp} \gg V_{||} \sim 0$. In general, it is found that when the parallel resistivity and the parallel viscosity are negligible with respect to the corresponding perpendicular coefficients, the growth rates display a weaker power law dependence on the surviving dissipative coefficient than in the corresponding "isotropic" case. Also the dependence on the wavelength changes in the corresponding dispersion relations.

The lower half of Table I displays the scalings of the fastest growing mode, which we have numerically obtained. They coincide, like for the reduced-MHD case, with the estimates that can be deduced^{11,13} by balancing $\delta_{LD}(k_M) \sim \delta_{SD}(k_M)$ or $\gamma_{LD}(k_M) \sim \gamma_{SD}(k_M)$, so to find the scaling of k_M and therefore that of δ_M and of γ_M . These results are of potential interest for reconnection in large aspect ratio current sheets –arguably in some electron-only reconnection regimes observed in turbulence (cf. Sec. V). In previous works on EMHD tearing modes, they had been provided only in the inertia-driven regime¹¹ and, partially, in the resistive regime⁸. The numerical results we have here obtained in the collisionless regime provide a correction to the estimates of Ref. 11 but confirm the numerical results therein obtained, for which a discrepancy from theoretical estimates, based on previous scalings available in literature⁶, had been remarked. Our result differ instead from the previous scalings of the resistive case⁸.

It is interesting to note that, once the scalings of the growth rates and of the reconnection layer are expressed using the heuristic arguments presented in Sec. IV, the scalings of each quantity are formally identical in both the small- and large- Δ' limits in any one-parameter regime considered in the following (cf., e.g., Eqs. (39, 44, 48, 56, 56) next): the scalings obtained in the different wave-length limits are thus entirely determined by the specific scaling that $l_c \sim (D')^{-1}$ gets in the small- and large- Δ' limits. This "symmetry" in the dispersion relation had been already noted in Ref. 14 for tearing modes in reduced MHD, where D' can be replaced by Δ'_{vy} (see Appendix F therein). As a remarkable consequence, it turns out that both conditions $\delta_{LD}(k_M) \sim \delta_{SD}(k_M)$ and $\gamma_{LD}(k_M) \sim \gamma_{SD}(k_M)$, when they are non-trivial, lead to the unique condition

$$D'_{LD}[k_M] \sim D'_{SD}[k_M]. \quad (35)$$

The latter, once more, highlights the usefulness of having introduced the characteristic scale length D' , together with a numerical procedure for evaluating it.

Finally, the last line at bottom of Table I shows the asymptotic scaling that the inverse critical aspect ratio a/L of the current sheet must have in order to give a growth rate of order unity, once the reference length is assumed to be $L_0 = L$, rather than $L_0 = a$. This is likely to occur for secondary tearing modes. The critical value $(a/L)_{crit}$ correspond to the threshold for the "ideal tearing" condition of Ref. 112, below which the current sheet is abruptly disrupted over the ideal time scales of evolution of the system. Note that in assuming $L_0 = L$ also the reference time τ_w must be rescaled to $\tau_w^* = \tau_w(a/L)^2$. Below and in the table, the apex "*" labels quantities for which the normalization scale is $L_0 = L$, instead of $L_0 = a$. The scaling of the last line have not been numerically obtained like it has been done, e.g., in Refs.11, 98, 110, and 112, but are deduced from the other scalings by imposing $\gamma_M \tau_w^* \sim O(1)$.

It should be finally noted that the previously available theoretical scalings in the purely collisionless⁶ and in the purely viscous¹⁰ cases had been obtained by relying on the same kind of boundary layer calculations and approximations first detailed in Ref. 6. The different results we have numerically found, and which we believe to be more accurate, are instead supported by the heuristic analysis outlined in Sec. IV A. In some respect the latter could be considered "less rigorous" or at least, more prone to false assumptions than the approximations and orderings required by the boundary layer approach, on which the previous theoretical results are grounded —this difference had been explicitly discussed, for example, in the reduced-MHD context in Ref.

14. Nevertheless, we will see that the heuristic approach discussed above agrees with the numerical results in cases in which the difference with respect to the theoretical estimates is quite evident. At the same time, we will see that the same heuristic analysis even plays a crucial role in the quantification of the power-law scalings, in cases in which discriminating univocally between fractions like $7/32$ and $1/4$ from the fit of the numerical data would not be possible, otherwise: the key point we want to emphasize, here, is the global coherence displayed by the combination of the numerical estimates *and* of the heuristic analysis in both the small- and large- Δ' limits and in the wavelength range of the fastest growing mode, in all reconnection regimes we have investigated. This supports the result we have found, also when they differ from previous theoretical estimates and, in our opinion, provides an a posteriori verification of the correctness –or at least consistency– of the heuristic assumptions we made.

A. Collisionless, inertia-driven regime

In this regime we can assume $\psi_1|_\delta \sim d_e^2 \psi_1''|_\delta$, which gives

$$d_e^2 \sim l_c \delta, \quad (36)$$

and $b_1|_\delta \ll d_e^2 b_1''|_\delta$. Combining the appropriate limit of Eq.(26),

$$\gamma d_e^2 b_1''|_\delta \sim k \delta \psi_1''|_\delta, \quad (37)$$

with Eq.(27) and with Eq.(28), one finds

$$d_e^2 \frac{\gamma^2}{k^2 \delta^2} \frac{1}{\delta^2} \sim \frac{1}{l_c \delta} \Rightarrow \gamma \sim k \frac{\delta^2}{d_e^2}. \quad (38)$$

Combining the latter with Eq.(36) so to eliminate δ and using then the first of conditions (29) we find

$$\gamma \sim k d_e^2 (D')^2, \quad \delta \sim d_e^2 D'. \quad (39)$$

This writing is useful since numerical integration shows that the scaling of D' is not trivial. The coherence of the relations in Eqs. (38) can be verified using the scalings, numerically obtained by scanning a wide parameter range, which are shown in Fig. 1: the scaling laws of γ (which are $\sim d_e^2$

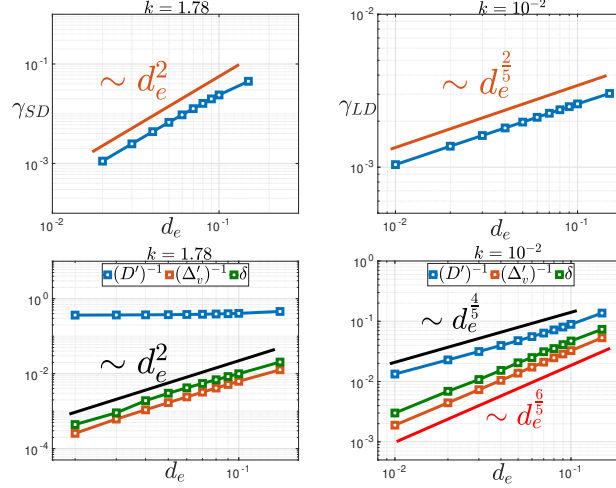


FIG. 1. Numerical results of the linear analysis in the small- Δ' limit (left frames) and in the large- Δ' limit (right frames) for the purely collisionless EMHD tearing mode. The growth rate scalings expressed as a function of the electron skin depth are in the top frames, while the scalings of $(D')^{-1}$, of $(\Delta'_y)^{-1}$ and of δ are in the bottom frames. A departure from the power-law scaling is visible for $d_e \gtrsim 0.1$ (cf. also Table II).

and $\sim d_e^{2/5}$ for small- and large- Δ' limits in the top-left and the top-right frames, respectively), and also of the scale lengths $(D')^{-1}$, $(\Delta'_y)^{-1}$ and δ with respect to d_e are here shown in both the small- Δ' (left frames) and large- Δ' (right frames) wavelength limits. The overall results are summarized in the first column of Table I. They complement and correct the analytical estimates first obtained in Refs.3, 5–7 via boundary layer integration (some discrepancies between theoretical estimates and numerical integration had been already noted in Ref. 12). For illustrative purposes, the spatial profiles of the eigenfunctions ψ and b are shown in Fig. 2: for the small- Δ' limit, a case with $d_e = 0.05$ and $k = 0.01$ is shown (left frames); for the large- Δ' limit a case with $d_e = 0.021$ and $k = 2.1$ is shown (right frames). Qualitatively analogous spatial profiles –which will not be shown in this manuscript– are obtained also for the resistive and viscous cases, which will be discussed next).

The wave-number of the fastest growing mode follows therefore from balancing, for example, either the layer widths ($\delta_{LD}(k_M) \sim \delta_{SD}(k_M)$) or the growth rates ($\gamma_{LD}(k_M) \sim \gamma_{SD}(k_M)$) for $\Delta' \sim k^{-p}$. In both cases one has to solve the condition (35): this yields $d_e^{6/5} \sim d_e^2 k_M^{-p}$, which gives $k_M \sim d_e^{4/(5p)}$ and therefore $\gamma_M \sim d_e^{(4+2p)/(5p)}$. Using this scaling and changing the normalization length scale to $L_0 = L$, one obtains $(a/L)^2 \gamma_M \tau_w^* \sim (d_e^*)^{(4+2p)/(5p)} (L/a)^{(4+2p)/(5p)}$. The condition $\gamma_M \tau_w^* \sim 1$ implies

$$\left(\frac{a}{L}\right)_{crit} \sim (d_e^*)^{\frac{2+p}{2+6p}}. \quad (40)$$

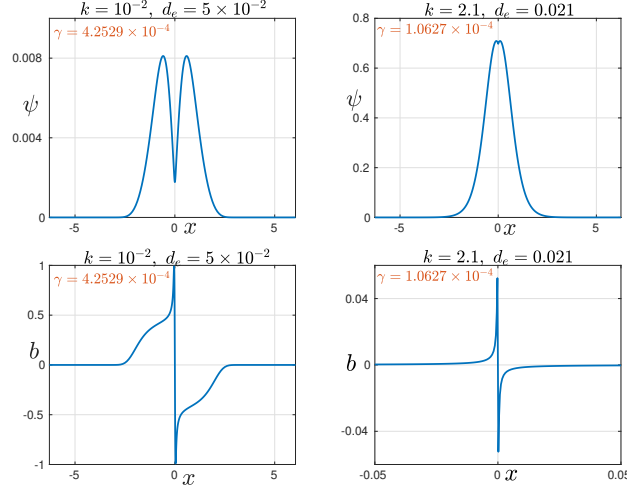


FIG. 2. Spatial profile of the eigenfunctions ψ (top frames) and b (bottom frames) for a small- Δ' limit case with $d_e = 0.05$ and $k = 0.01$ (left frames) and for a large- Δ' limit case with $d_e = 0.021$ and $k = 2.1$ (right frames).

Note that condition (40) corrects the theoretical estimate $(a/L)_{crit} \sim (d_e^*)^{(3+2p)/(6+8p)}$ of Eq.(17) of Ref. 11, which had been obtained by using indeed both the small- and large- Δ' estimates (36) and (37) of Ref.6, where, beside of the discrepancy with respect to the large- Δ' limit here found, the dependence on k in the small- Δ' limit had been neglected.

Remarkably, for $p = 1$, the threshold condition (40) coincides with the result $(a/L)_{crit} \sim (d_e^*)^{3/8}$ that F. Pucci numerically obtained in the work of Ref. 11 for a Harris pinch equilibrium ($\psi_0 = B_0 a \tanh(x/a)$, which indeed has $p = 1$) by using an adapted version of the solver of Ref. 112: this value was therein taken as the best estimate of the threshold condition to the “ideal tearing” regime in collisionless EMHD (cf. with Fig.2 and with comments between Eqs.(17) and (18), therein), in slight disagreement with the theoretical estimate there obtained from the previous collisionless EMHD scaling available in literature for the large- and small- Δ' limits. This fact is in further support of the scaling in the large- Δ' limit that we have numerically obtained, here.

We also note that, thanks to the writing of Eq. (39), both the conditions $\gamma_{LD}(k_M) \sim \gamma_{SD}(k_M)$ and $\delta_{LD}(k_M) \sim \delta_{SD}(k_M)$, when they are not trivial, translate into the unique condition $(D'_{LD}[k_M]) \sim (D'_{SD}[k_M])$. As we will see, this condition is common to all the one-parameter regimes that we are going to consider in this Section.

B. Resistive regime with $R_{||} = \mathcal{A}R_{\perp}$

In the light of a heuristic interpretation, from the appropriate limit of (25) we obtain, after balancing the first and last term,

$$\gamma \sim \frac{R_{\perp}}{l_c \delta}. \quad (41)$$

Combining Eq.(27) with the equivalent of (37) obtained from (26), that is,

$$k\delta\psi_1''|_{\delta} \sim R_{||}b_1''|_{\delta}, \quad (42)$$

and using again Eqs.(28,27), one finds

$$k\delta \frac{1}{\delta l_c} \sim \frac{R_{||}}{\delta^2} \frac{\gamma}{k\delta} \implies \gamma \sim \frac{k^2 \delta^3}{l_c \mathcal{A} R_{\perp}}, \quad (43)$$

having used $R_{||} = \mathcal{A}R_{\perp}$ in the last passage. One can then use once more (41) so to alternatively eliminate δ and γ : combined with the first of Eqs. (29), i.e., $l_c \sim 1/D'$, this gives, respectively,

$$\gamma \sim k^{\frac{1}{2}} \mathcal{A}^{-\frac{1}{4}} R_{\perp}^{\frac{1}{2}} D', \quad \delta \sim k^{-\frac{1}{2}} \mathcal{A}^{\frac{1}{4}} R_{\perp}^{\frac{1}{2}}. \quad (44)$$

It should be noted that the scalings of δ are here identical for both the small and the large wave-length limits.

The scalings (44), included their dependence on \mathcal{B} , are numerically confirmed. This is shown in Fig.3, for what concerns the dependence on R_{\perp} : in the top frame we show the scalings of γ with R_{\perp} for $\mathcal{A} = 1/2$; the scalings in the center and bottom frames correspond instead to the isotropic case with $\mathcal{A} = 1$, i.e., $R_{||} = R_{\perp} = R$. The scalings in the second column of Table I are obtained after numerically verifying that $(D')_{LD} \sim k^{1/3} R^{-1/3}$ and $(D')_{SD} \sim \Delta'$ (their dependence on R_{\perp} is shown in the bottom frame of the aforementioned figure). It can be noted that all the results for the isotropic resistive case $R_{||} = R_{\perp} = R$ can be recovered from the inertia-driven case, by formally substituting $\gamma d_e^2 \rightarrow R$.

The scalings of δ and γ obtained in the small- Δ' limit in Ref. 2, 3, 7, and 12 are thus recovered. In this wave-length limit we also (numerically) verify that $\delta \sim (\Delta'_{vy})^{-1}$.

The scalings (44) also coincide with the analytical result of Shaikhislamov⁸ for what concerns δ evaluated in the large- Δ' limit, but the corresponding growth rate $\gamma \sim k^{3/4} R^{1/4}$ therein obtained

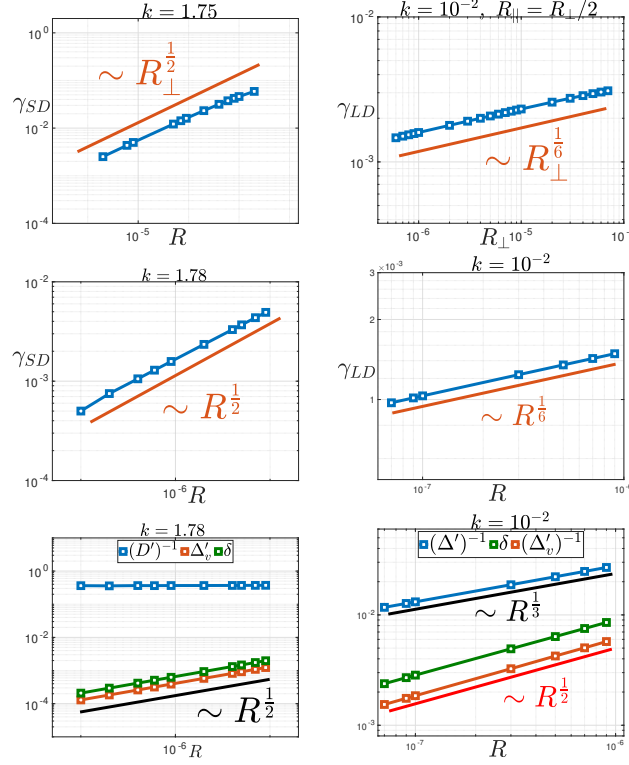


FIG. 3. Numerical results of the linear analysis in the small- Δ' limit (left frames) and in the large- Δ' limit (right frames) for the purely resistive EMHD tearing mode with $R_{||} = R_{\perp}/2$ (top frames) and with $R = R_{\perp} = R_{||}$ (center and bottom frames). Only the scalings of the growth rate are shown for the case $R_{||} = R_{\perp}/2$ for comparison, since the same power laws of the $R = R_{\perp} = R_{||}$ are obtained also for $(D')^{-1}$, of $(\Delta'_v)^{-1}$ and of δ (shown in the center frame): the proportionality factor $\mathcal{A} = 0.5$ only determines a re-scaling of each quantity by a factor close to one. Note the slight departure from the asymptotic power law as the non-ideal parameters approach the limit of validity of the boundary layer theory (rightmost "diamonds" approaching or overtaking $R \sim 10^{-5}$ –cf. the center column of Table II).

for $ka \ll 1$ differs with respect to the scaling $\gamma_{LD} \sim k^{5/6} R^{1/6}$ we obtain numerically and according to Eqs.(44).

This time, the scaling of the fastest growing mode can not be recovered by balancing $\delta_{LD} \sim \delta_{SD}$, since the two scalings are identical, but it can be rather obtained from $\gamma_{LD}(k_M) \sim \gamma_{SD}(k_M)$. In any case we rely on Eq. (35), using the numerical scalings obtained for D' in the two wavelength limits. This yields $k_M \sim R^{1/(1+3p)}$ and therefore $\gamma_M \sim R^{(2+p)/(2(1+3p))}$ and $\delta_M \sim R^{3p/(2(1+3p))}$. These estimates agree with the scaling laws of the fastest growing modes, which we have obtained numerically and which for $p = 2$ are shown for both γ_M and δ_M in the top-left- and top-right frames of Fig.4, respectively. The analytical estimates $k_M \sim R^{1/6}$ and $\gamma_M \sim R^{1/3}$ suggested in Ref. 8 differ from those we have obtained for both the cases $p = 1$ and $p = 2$ (although the dependence on the equilibrium choice had not been noted, in that work).

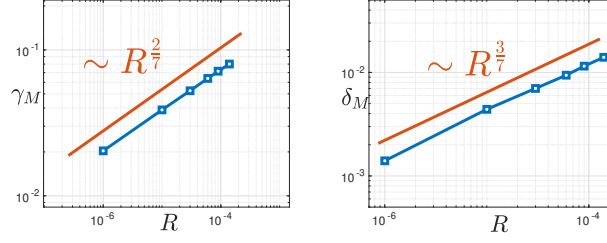


FIG. 4. Growth rates (left frames) and widths of reconnecting layer (right frames) of the fastest growing modes for resistive EMHD modes with respect to R_\perp for $R_\parallel = R_\perp$.

Naming then R^* the quantity R evaluated for $L_0 = L$ and using the fact that $R^* = R$ (cf. first of Eqs. (12) and the definition of τ_w) we write $(a/L)^2 \gamma_M \tau_w^* \sim (R^*)^{(2+p)/(2(1+3p))}$, which for $\gamma_M \tau_w^* \sim 1$ yields

$$\left(\frac{a}{L}\right)_{crit} \sim (R^*)^{\frac{2+p}{4(1+3p)}} \quad (45)$$

C. Resistive regime with $R_\perp \neq 0$ and $R_\parallel = 0$

Since generally $R_\perp \sim R_\parallel$ (cf. Eq. (34)), this regime is meaningful just from a theoretical point of view, in the measure it provides the scalings in the formal limit $R_\parallel \rightarrow 0$, which can be potentially useful as a benchmark limit test for theoretical models. In this regime the equations are the same of the previous case, except for the relevant limit of Eq.(26). Therefore, the same conditions provided by Eqs.(27) and (41) hold. Eq.(51) is instead replaced by

$$\gamma b_1|_\delta \sim k \delta \psi_1''|_\delta, \quad (46)$$

which gives

$$\frac{\gamma^2}{k^2 \delta^2} \sim \frac{1}{\delta l_c} \Rightarrow \delta^3 \sim \frac{k^{-2} R^2}{l_c}. \quad (47)$$

The second of Eqs.(47) is obtained from the former after using (41). Therefore, combining them so to eliminate δ in the expression of γ and using the first of Eqs. (29), i.e., $l_c \sim 1/D'$, we can write the following general estimates, in principle valid in both wave-length limits:

$$\gamma \sim k^{2/3} R^{1/3} (D')^{2/3}, \quad \delta \sim k^{-2/3} R^{2/3} (D')^{1/3}. \quad (48)$$

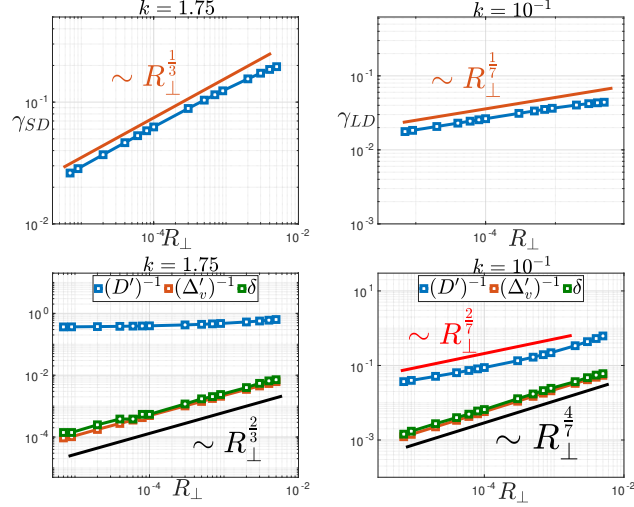


FIG. 5. Growth rates (upper frames) and scaling of some characteristic lengths (lower frames) of resistive EMHD modes with respect to R_{\perp} for $R_{\parallel} = 0$ in the small- Δ' limit (left frames) and in the large- Δ' limit (right frames). A departure from the power-law is visible for $R_{\perp} \gtrsim 10^{-3}$ (four rightmost "diamonds" in any frame).

After numerical integration, here again, we obtain $D' \sim \Delta'$ and $\Delta_{vy} \sim \delta^{-1}$ in the small- Δ' limit, and $(\Delta'_{vy})^{-1} \sim \delta^{-1}$ and a non-trivial scaling $D' \sim R^{-2/7}$ in the large- Δ' limit, whence the results in the table follow. In this regime, as it is reported in Table I, the scalings of the growth rate and of the reconnecting layer width differ in both the small- and in the large- Δ' limits from those previously discussed for the "isotropic resistive" case $R_{\perp} = R_{\parallel}$. Their scaling, numerically obtained, are shown in Fig.5, although with respect to their dependence on R_{\perp} alone: $\gamma_{LD} \propto R_{\perp}^{1/7}$, $\delta_{LD} \propto R_{\perp}^{4/7}$, $\gamma_{SD} \propto R_{\perp}^{1/3}$, and $\delta_{SD} \propto R_{\perp}^{2/3}$.

By following the same line of thoughts of the previous section, the scaling laws of the fastest growing mode can be obtained from Eq. (35). This leads to $k_M \sim R_{\perp}^{2/7p}$, $\gamma_M \sim R_{\perp}^{(4+3p)/21p}$, and $\delta_M \sim R_{\perp}^{(12p-4)/21p}$. These scalings for the fastest modes are shown on the bottom frames of Fig.4. By looking at the scalings of fastest modes in Fig.4, one sees that the inclusion of non-vanishing R_{\parallel} leads to a slight decrease in the growth rate with respect to R_{\perp} .

The critical aspect ratio in this regime reads

$$\left(\frac{a}{L}\right)_{crit} \sim (R_{\perp}^*)^{\frac{4+3p}{42p}}, \quad (49)$$

where $R_{\perp}^* = R_{\perp}$.

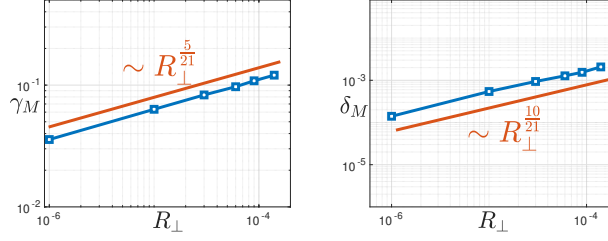


FIG. 6. Growth rates (left frames) and widths of reconnecting layer (right frames) of the fastest growing modes for resistive EMHD modes with respect to $R_{\perp} \neq 0$ for $R_{\parallel} = 0$.

D. Viscous regime with $V_{\parallel} = \mathcal{B}V_{\perp}$

In this regime, beside of Eq.(27) we obtain from Eq.(25),

$$\gamma \sim \frac{V_{\perp}}{l_c \delta^3}. \quad (50)$$

Eq.(26) reduces to

$$k \delta \psi_1''|_{\delta} \sim V_{\parallel} b_1^{iv}|_{\delta}, \quad (51)$$

which, using (28,29) and (27), yields

$$\gamma \sim k^2 \delta^5 D' V_{\parallel}^{-1}. \quad (52)$$

Using now $V_{\parallel} = \mathcal{B}V_{\perp}$ and eliminating γ thanks to Eq. (29), one obtains

$$\gamma \sim k^{3/4} \mathcal{B}^{5/8} V_{\perp}^{1/4} D', \quad \delta \sim k^{-1/4} \mathcal{B}^{1/8} V_{\perp}^{1/4}. \quad (53)$$

Similarly to the resistive case with $R_{\parallel} \propto R_{\perp}$, the scalings of δ are identical for both the small and the large wavelength limits.

All the scalings in the table are thus recovered numerically: in the small- Δ' limit for $D' \sim \Delta'$ and $\Delta'_{v_y} \sim \delta^{-1}$, and in the large- Δ' limit for the non-trivial scaling numerically obtained for D' (i.e., $D' \sim k^{1/4} V^{-1/6}$) and for $\Delta'_{v_y} \sim \delta^{-1}$. This is confirmed by the numerical results. The dependence of the intrinsic scale lengths and of the growth rates on V (i.e., $\gamma_{SD} \propto V^{1/4}$ and $\gamma_{LD} \propto V^{1/12}$) are shown in Fig.7 for the "isotropic viscous case" case $V_{\parallel} = V_{\perp} = V$. These results agree with the theoretical predictions of the growth rates obtained by Avinash et al.⁵ and by Cai and Li¹⁰ in the small- Δ' limit. However, they differ from their results in the large- Δ' limit, where $\gamma \sim k^{7/8} V^{1/8}$

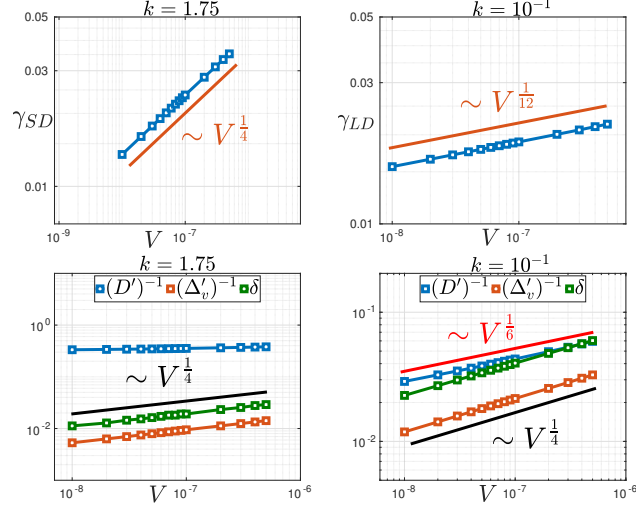


FIG. 7. Numerical results of the linear analysis in the small- Δ' limit (left frames) and in the large- Δ' limit (right frames) for "isotropic" viscous EMHD tearing mode with respect to $V = V_{\perp} = V_{\parallel}$. The growth rates scaling of γ are in the top frames, while the scalings of $(D')^{-1}$, of $(\Delta'_v)^{-1}$ and of δ are in the bottom frames.

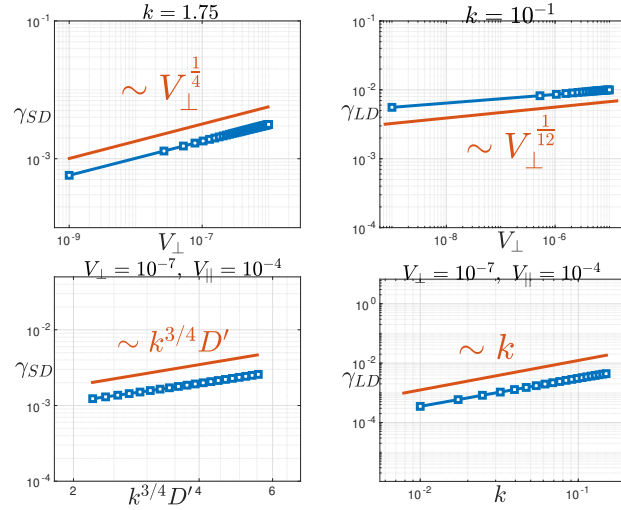


FIG. 8. Scaling laws in the small- Δ' (left frames) and large- Δ' (right frames) limits as a function of V_{\perp} (top frames) and as a function of the wavenumber k (bottom frames) for the case $V_{\perp} = 10^{-3}V_{\parallel}$.

868 and $\delta \sim k^{-7/32}V^{7/32}$ (therein implicitly given via the relation $V \sim \gamma\delta^4$) have been obtained, in
 869 place of the scalings $\gamma_{LD} \sim kV^{1/12}$ and $\delta_{LD} \sim k^{-1/4}V^{1/4}$, which we have found. For comparison,
 870 the scalings of γ obtained in the small- and large- Δ' limits in the case $\mathcal{B} = 10^3$ are shown in Fig.
 871 8: these are identical to those of the $\mathcal{B} = 1$ case (Fig. 7), except for a rescaling factor in the
 872 amplitude, corresponding to the factor $\mathcal{B}^{5/8}$ for γ and $\mathcal{B}^{1/8}$ for δ (cf. Eqs. 56).

873 Following the matching condition of Eq. (35), the scaling laws of the fastest mode are then
 874 found to be $k_M \sim V^{2/(3+12p)}$, $\gamma_M \sim V^{(4p+9)/(12+48p)}$, and $\delta_M \sim V^{(1+12p)/(12(1+4p))}$. The scaling

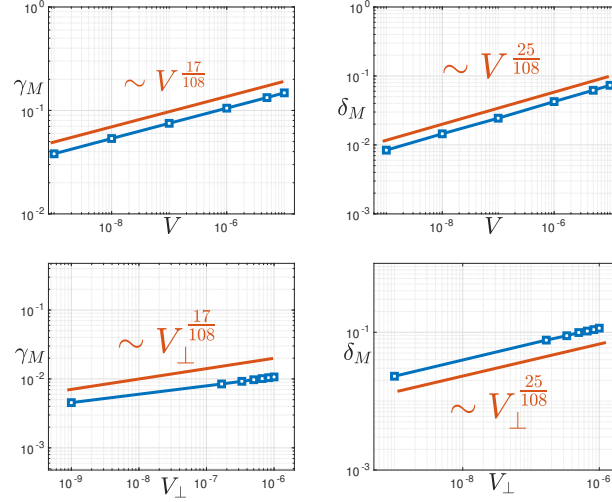


FIG. 9. Growth rate scaling of the fastest growing modes for viscous EMHD modes and with respect to $V = V_\parallel = V_\perp$ (top frames) and with respect to V_\perp for $V_\parallel = 10^3 V_\perp$ (bottom frames): the asymptotic scaling is identical in both cases, the factor $\mathcal{B} = 10^3$ only affects the reference amplitude via the proportionality factors $\mathcal{B}^{5/8}$ and $\mathcal{B}^{1/8}$, respectively, according to Eqs. (56).

numerically obtained for the magnetic equilibrium corresponding to $p = 2$ and shown in the top panels of Fig.9 for both the cases $\mathcal{B} = 1$ and $\mathcal{B} = 10^3$ agree with these predictions. In this regard it should be however emphasized the crucial role that the heuristic analysis has played in quantifying the scaling shown in Fig. 7: it is practically impossible to distinguish from a numerical fit, a scaling $17/108$ from –for example– the value $1/6 = 18/108$. Because of this, the numerical results shown in the top frames of Fig. 7 should be read as a whole, together with those in the small- and large- Δ' limits and in the light of Eqs. (56): it is indeed thanks to the consistency they display with the results in the small and large wavelength limits and with the heuristic argument we have used to obtain the fastest growing mode, that take them as reliable –although, rigorously speaking, should we read the numerical results separately, they would not exclude an infinity of numerically close fractional scalings. These issues will be even more evident in the regime we will discuss next.

Naming V^* the quantity V evaluated for $L_0 = L$ and using $V^* = (a/L)^2 V$ according to Eqs. (12) and to the definition of τ_w , we can write $(a/L)^2 \gamma_M \tau_w^* \sim (V^*)^{(4p+9)/(12+48p)} (L/a)^{(4p+9)/(6+24p)}$, which for $\gamma_M \tau_w^* \sim 1$ yields

$$\left(\frac{a}{L}\right)_{crit} \sim (V^*)^{\frac{9+4p}{42+104p}} \quad (54)$$

E. Viscous regime with $V_{\perp} \neq 0$ and $V_{\parallel} = 0$

Like for the "anisotropic resistive" regime of Sec. VIC, the interest in this anisotropic viscous regime, too, is mostly theoretical, since the opposite case $V_{\parallel} \gg V_{\perp}$ is the one which is typically of experimental interest (cf. Sec. V). Nevertheless, knowing the scalings in the formal limit $V_{\parallel} \rightarrow 0$, can be useful as a benchmark limit test for theoretical models in which a mani-parameter dependence is considered.

Similarly to what happen in the resistive regime, in this case Eq.(50) is unchanged whereas Eq.(51) is replaced by Eq.(46), provided the substitutions $V \rightarrow V_{\perp}$. Combining then (50) with Eqs.(28), (27) and (46), one obtains

$$\delta^7 \sim \frac{k^{-2} V_{\perp}^2}{l_c}. \quad (55)$$

Therefore, using again (29) and (50), we can write

$$\gamma \sim k^{6/7} V_{\perp}^{1/7} (D')^{4/7}, \quad \delta \sim k^{-2/7} V_{\perp}^{2/7} (D')^{1/7}. \quad (56)$$

In the small- Δ' limit we numerically find $D' \sim \Delta'$ and $\Delta'_{v_y} \sim \delta^{-1} \propto V_{\perp}^{-2/7}$, and in the large- Δ' we find $D' \sim V_{\perp}^{-1/8}$ and $\Delta'_{v_y} \sim \delta^{-1}$. The scaling dependence on V_{\perp} , numerically verified for these quantities, is shown in the bottom frames of Fig.10 (the dependence on k are not shown, here) together with the $\gamma_{LD} \propto V_{\perp}^{1/14}$ and $\gamma_{SD} \propto V_{\perp}^{1/7}$ dependence found for the growth rates. The complete scalings on both V_{\perp} and k are reported in the Table I.

In this regard we must comment about the $\Delta'_{v_y} \sim \delta^{-1} \propto V_{\perp}^{-15/56}$ scaling shown in Figure 10 and reported in Table I, for which the same arguments discussed in previous Section (VID) for the scaling of the fastest growing mode hold: one could question about the accuracy of this estimate, since $15/56 \simeq 0.268 \pm 0.0005$ is very close, for example, to the fractional value $1/4$ (actually, within a 6.7% relative error). The reason for which we opted to report the fractional value $15/56$ for the exponent of V_{\perp} is indeed that this numerical value is coherent with the heuristic-type analysis discussed in Sec. IV and which we have shown to work well in all regimes discussed so far: the exponent $15/56$ in the scaling of δ_{LD} is indeed the value obtained by substituting $l_c = (D')_{LD}^{-1} \sim V_{\perp}^{-1/8}$ in Eq.(55), which is also the scaling which, once substituted in the first of Eqs. (56), gives $\gamma_{LD} \propto V_{\perp}^{1/14}$. If, instead, had one taken the scaling $(D')_{LD}^{-1} \sim V_{\perp}^{-1/4}$, according to Eq. (56) this would have given a growth rate independent on V_{\perp} , which is not reasonable, since we must have $\gamma(V_{\perp}) \rightarrow 0$ as $V_{\perp} \rightarrow 0$.

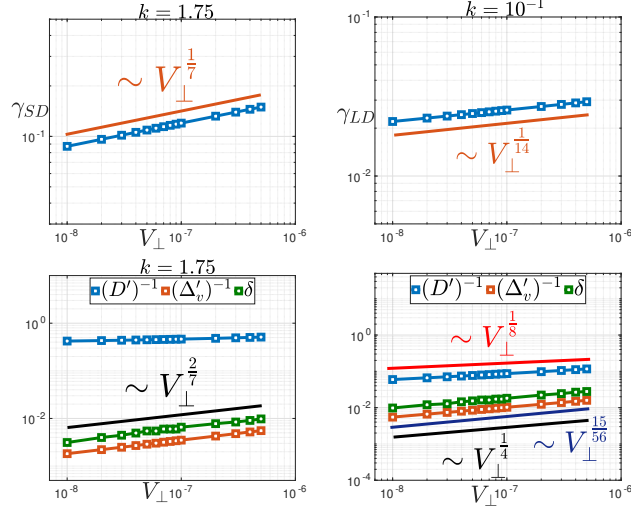


FIG. 10. Numerical results of the linear analysis in the small- Δ' limit (left frames) and in the large- Δ' limit (right frames) for viscous EMHD tearing mode with $V_{\perp} \neq 0$ and $V_{\parallel} = 0$. The growth rates scaling as function of V_{\perp} are in the top frames, while the scalings of $(D')^{-1}$, of $(\Delta'_v)^{-1}$ and of δ are in the bottom frames.

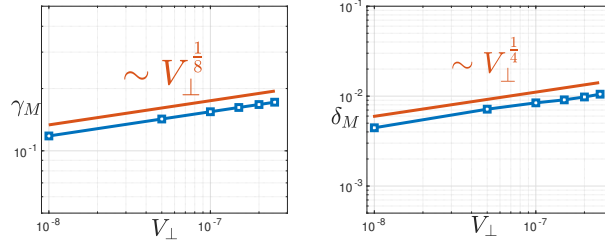


FIG. 11. Growth rate scaling of the fastest growing modes for viscous EMHD modes with respect to V_{\perp} in the $V_{\perp} \neq 0$, $V_{\parallel} = 0$ case .

Moreover, as a further consistency check, we notice that all this is coherent with the scaling laws of the fastest growing mode obtained by applying the matching criterion $D'_{LD}(k_M) \sim D'_{SD}(k_M)$ for $D'_{LD} \sim V_{\perp}^{-1/8}$. This yields $k_M \sim V_{\perp}^{1/8p}$, $\gamma_M \sim V_{\perp}^{(2p+3)/(28p)}$, and $\delta_M \sim V_{\perp}^{(15p-2)/(56p)}$. The agreement of these estimates with the numerical results is shown in the bottom frames of Fig.11, where they have been numerically verified for the equilibrium (20). Using $V_{\perp}^* = V_{\perp}(a/L)^2$ the critical aspect ratio for this regime reads

$$\left(\frac{a}{L}\right)_{crit} \sim (V_{\perp}^*)^{\frac{3+2p}{6+60p}}. \quad (57)$$

VII. CONCLUSIONS

Using an adapted version of the linear solver of Ref. 13 we have revised the scalings of incompressible EMHD tearing modes when they depend on a single parameter (Sec. VI). The latter has been chosen to be, respectively, the normalized electron skin depth (related to a finite electron inertia — Sec. VIA), the perpendicular resistivity (related to electron ion-collisions — Sec. VIB) and the perpendicular electron viscosity (see Sec. VID). We have considered not only the cases in which the parallel resistivity and viscosity are proportional to the perpendicular counterparts, but also the cases in which the parallel resistivity and viscosity are respectively set to zero (see Sec. VIC, VIE): although of more theoretical interest, these latter cases can be useful to test the convergence of more complete analytical models in some regimes (see Sec. V). The analysis we have performed has spanned both the large- and small wavelength limits, respectively related to the small- and large- Δ' limits, and included also the study of the scalings of the fastest growing mode, which can be formally destabilized in a continuum spectrum of unstable modes. The latter condition is likely to occur in a large enough aspect ratio current sheet, which for EMHD tearing modes we argue to be relevant to the "electron-only" regime (Sec. III), in recent literature identified to occur in the nonlinear development of Alfvénic reconnection. All the results we have obtained are summarized in Table I.

The scalings in the small- and large- Δ' limits had been already estimated with analytical models in the purely inertial regime^{3,6}, in the purely resistive isotropic regime^{2,3,8} and in the purely viscous isotropic regime^{5,10}: while the numerical study we have performed recovers the results already available in literature for the small- Δ' limits, a different scaling is numerically found with respect to previous estimates provided in all large- Δ' limits (except for the scaling of the reconnecting layer width provided in Ref. 8 for the isotropic resistive regime). All the results we have obtained have been interpreted by means of a heuristic analysis performed in terms of some "new" characteristic scale lengths associated to the gradients of the eigenfunctions, which have been first introduced in Ref. 14 and which must be numerically evaluated. The scalings of the fastest growing mode have been previously considered only in the purely isotropic resistive regime⁸ and in the purely collisionless regime¹¹. However, the numerical results we obtained in the former one, do not agree with previous analytical estimates. The numerical results we found in the collisionless regime, on the other hand, coincide with the numerical results already found in Ref. 11 and disagree with the theoretical estimates, which in the same work had been already noticed to slightly depart from

the numerical scaling. Interestingly, all these findings can be interpreted in a coherent way, in the framework of the heuristic analysis we have provided.

We conclude by noting the crucial role played in this work by the combination of *both* the numerical analysis *and* the heuristic estimates: while the former is capable, in some regimes, to give unambiguous results, which a posteriori support the heuristic-type analytical derivation of the scaling laws, in other regimes it is only thanks to the heuristic estimates, that specific power law scalings can be singled out from the fit of the numerical data, which, otherwise, would be compatible with several different fractional scalings that are numerically too close one to each other to be unambiguously distinguished one from another. The global coherence provided by the combination of both approaches, especially in the verification of the scalings of the fastest growing mode by using those obtained in the small- and large- Δ' limits, strongly supports the results we have obtained, also when they depart from previous analytical estimates obtained using a boundary layer integration.

The one-parameter study we developed here will be extended to a two parameter-study in regimes of relevance for experimental cases, in a future dedicated work.

ACKNOWLEDGMENTS

This work has been carried out within the framework of the French Federation for Magnetic Fusion Studies (FR-FCM) and of the Eurofusion consortium, and has received funding from the Euratom research and training programme 2014-2018 and 2019-2020 under grant agreement No 633053 (WPEDU fundings obtained through FR-FCM AAP 2017-2021 “Evolution of current sheets in low-collision plasmas”, in particular, are gratefully acknowledged). The views and opinions expressed herein do not necessarily reflect those of the European Commission. During the completion phase of this work, one of the authors (H.B., formerly at IJL in Nancy) has received financial support from the AIM4EP project (ANR-21-CE30-0018), funded by the French National Research Agency (ANR). The authors wish to thank E. Tassi, C. Granier, D. Laveder and T. Passot (Observatoire de la Cote d’Azur, Nice) for interesting discussions had with them while this work was under peer-review, and which have inspired to us the inclusion of Table II in the final version of this manuscript.

VIII. DATA AVAILABILITY

The data that supports the findings of this study are available within the article.

REFERENCES

- ¹H. P. Furth, J. Killeen, and M. N. Rosenbluth, “Finite-resistivity instabilities of a sheet pinch,” *Phys. Fluids* **6**, 459–484 (1963).
- ²A. V. Gordeev, “Stability of a plasma contained by a strongly non-uniform magnetic field,” *Nucl. Fusion* **10**, 319 (1970).
- ³S. V. Bulanov and A. S. Pegoraro, F. and Sakharov, “Magnetic reconnection in electron magnetohydrodynamics,” *Phys. Fluids* **8**, 2499–2508 (1992).
- ⁴A. Fruchtman and H. R. Strauss, “Modification of short scale-length tearing modes by the hall field,” *Phys. Fluids B* **5**, 1408 (1993).
- ⁵K. Avinash, S. V. Bulanov, T. Esirkepov, P. Kaw, F. Pegoraro, P. V. Sasorov, and A. Sen, “Forced magnetic field line reconnection in electron magnetohydrodynamics,” *Phys. Plasmas* **5**, 2849 (1998).
- ⁶N. Attico, F. Califano, and F. Pegoraro, “Fast collisionless reconnection in the whistler frequency range,” *Phys. Plasmas* **7**, 2381–2387 (2000).
- ⁷V. Mirnov, C. Hegna, and S. Prager, “Two-fluid tearing instability in force-free magnetic configuration,” *Phys. Plasmas* **11**, 4468–4482 (2004).
- ⁸Shaikhislamov, I. F., “Hall dynamics and resistive tearing instability,” *J. Plasma Phys.* **70**, 599 (2004).
- ⁹Shaikhislamov, I. F., “Collapse of the neutral current sheet and reconnection at micro-scales,” *J. Plasma Phys.* **74**, 215 (2008).
- ¹⁰H. Cai and D. Li, “Magnetic reconnection with electron viscosity in electron magnetohydrodynamics,” *Phys. Plasmas* **15**, 032301 (2008).
- ¹¹D. Del Sarto, F. Pucci, A. Tenerani, and M. Velli, ““ideal” tearing and the transition to fast reconnection in the weakly collisional MHD and EMHD regimes,” *J. Geophys. Res.- Space Phys.* **121**, 1857–1873 (2016).
- ¹²W. Guo, J. Wang, and D. Liu, “Numerical studies on electron magnetohydrodynamics tearing mode instability,” *AIP Advances* **11**, 115206 (2021).

- ¹³H. Betar, D. Del Sarto, M. Ottaviani, and A. Ghizzo, “Multiparametric study of tearing modes in thin current sheets,” *Phys. Plasmas* **27**, 102106 (2020).
- ¹⁴H. Betar, D. Del Sarto, M. Ottaviani, and A. Ghizzo, “Microscopic scales of linear tearing modes: a tutorial on boundary layer theory for magnetic reconnection,” *Journal of Plasma Physics* **88**, 925880601 (2022).
- ¹⁵Y. Kuramitsu, T. Moritaka, Y. Sakawa, T. Morita, T. Sano, M. Koenig, C. D. Gregory, N. Woolsey, K. Tomita, H. Takabe, Y. L. Liu, S. H. Chen, and M. Matsukiyo, S. amd Hoshino, “Magnetic reconnection driven by electron dynamics,” *Nature Comm.* **9**, 5109 (2018).
- ¹⁶T. D. Phan, J. P. Eastwood, M. A. Shay, J. F. Drake, B. U. Sonnerup, M. Fujimoto, P. A. Cassak, M. Øieroset, J. L. Burch, R. B. Torbert, A. C. Rager, J. C. Dorelli, D. J. Gershman, C. Pollock, P. S. Pyakurel, C. C. Haggerty, Y. Khotyaintsev, B. Lavraud, Y. Saito, M. Oka, R. E. Ergun, A. Retino, O. Le Contel, M. R. Argall, B. L. Giles, T. E. Moore, F. D. Wilder, R. J. Strangeway, C. T. Russell, P. A. Lindqvist, and W. Magnes, “Electron magnetic reconnection without ion coupling in earth’s turbulent magnetosheath,” *Nature* **557**, 202–206 (2018).
- ¹⁷J. E. Stawarz, J. P. Eastwood, T. D. Phan, I. L. Gingell, M. A. Shay, J. L. Burch, R. E. Ergun, B. L. Giles, D. J. Gershman, O. Le Contel, P.-A. Lindqvust, C. T. Russell, R. J. Strangeway, R. B. Torbert, M. R. Argall, D. Fischer, W. Magnes, and L. Franci, “Properties of the turbulence associated with electron-only magnetic reconnection in Earth’s magnetosheath,” *AstroPhys. J. Lett.* **877**, L37 (2019).
- ¹⁸P. S. Pyakurei, M. A. Shay, T. D. Phan, W. H. Matthaeus, J. F. Drake, J. M. TenBarge, C. C. Haggerty, K. G. Klein, P. A. Cassak, T. N. Parashar, M. Swisdak, and A. Chasapis, “Transition from ion-coupled to electron-only reconnection: basic physics and implications for plasma turbulence,” *Phys. Plasmas* **26**, 082307 (2019).
- ¹⁹A. Mallet, “The onset of electron-only reconnection,” *J. Plasma Phys.* **86** (2020).
- ²⁰F. Califano, S. S. Cerri, M. Faganello, D. Laveder, M. Sisti, and M. W. Kunz, “Electron-only reconnection in plasma turbulence,” *Frontiers in Physics* **8**, 317 (2020).
- ²¹H. Y. Man, M. Zhou, Y. Y. Yi, Z. H. Zhong, A. M. Tian, X. H. Deng, Y. Khotyaintsev, C. T. Russell, and B. L. Giles, “Observations of electron-only magnetic reconnection associated with macroscopic magnetic flux ropes,” *Geophys. Res. Lett.* **47**, e2020GL089659 (2020).
- ²²C. Vega, V. Roytershteyn, G. L. Delzanno, and S. Boldyrev, “Electron-only reconnection in kinetic-alfvén turbulence,” *Astrophysical J. Lett.* **893**, L10 (2020).

- ²³S. Lu, Q. Lu, R. Wang, P. L. Pritchett, M. Hubbert, Y. Qi, K. Huang, X. Li, and C. T. Russell,
“Electron-Only Reconnection as a Transition From Quiet Current Sheet to Standard Reconnection in Earth’s Magnetotail: Particle-In-Cell Simulation and Application to MMS Data,”
Geophys. Res. Lett. **49**, e2022GL098547 (2022).
- ²⁴J. M. Urrutia and R. L. Stenzel, “Helicon modes in uniform plasmas. i. low m ,” Phys. Rev. E **22**, 09211 (2015).
- ²⁵D. Del Sarto, F. Califano, and F. Pegoraro, “Pressure anisotropy and small spatial scales induced by velocity shear,” Phys. Rev. E **93**, 05303 (2016).
- ²⁶F. Pegoraro, B. S. V., F. Califano, and M. . Lontano, “Nonlinear development of the weibel instability and magnetic field generation in collisionless plasmas,” Phys. Plasmas **T63**, 262 (1996).
- ²⁷F. Califano, , F. Pegoraro, and B. S. V., “Spatial structure and time evolution of the weibel instability in collisionless inhomogeneous plasmas,” Phys. Rev. E **56**, 963 (1997).
- ²⁸F. Califano, , F. Pegoraro, B. S. V., and A. Mangeney, “Kinetic saturation of the weibel instability in a collisionless plasma,” Phys. Rev. E **57**, 7048 (1998).
- ²⁹F. Califano, D. Del Sarto, and F. Pegoraro, “Three-dimensional magnetic structures generated by the development of the filamentation (weibel) instability in the relativistic regime,” Phys. Rev. Lett. **96**, 105008 (2006).
- ³⁰A. Bret and C. Deutsch, “A fluid approach to linear beam plasma electromagnetic instabilities,” Phys. Plasmas **13**, 042106 (2006).
- ³¹M. Honda, “Eigenmodes and growth rates of relativistic current filamentation instability in a collisional plasma,” Physical Rev. E **69**, 016401 (2004).
- ³²F. Pegoraro, B. S. V., F. Califano, T. Z. Esirkepov, T. V. Lisejkina, M. Lontano, N. M. Naumova, H. Ruhl, A. S. Sakharov, and V. A. Vshivkov, “Coherent electromagnetic structures in relativistic plasmas,” Phys. Plasmas **7**, 889 (2000).
- ³³Y. J. Gu, S. V. Bulanov, G. Korn, and S. V. Bulanov, “Splitter target for controlling magnetic reconnection in relativistic laser plasma interactions,” Plasma Phys. Controll. Fusion **60**, 044020 (2018).
- ³⁴Y. J. Gu, O. Klimo, D. Kumar, Y. Liu, S. K. Singh, T. Z. Esirkepov, S. V. Bulanov, S. Weber, and G. Korn, “Fast magnetic field annihilation in the relativistic collisionless regime driven by two ultra-short high-intensity laser pulses,” Phys. Rev. E **93**, 013203 (2018).

- 1078 ³⁵Y. J. Gu, F. Pegoraro, P. V. Sasorovo, D. Golovin, A. Yogo, G. Korn, and S. V. Bulanov,
1079 “Electromagnetic burst generation during annihilation of magnetic field in relativistic laser-
1080 plasma interaction,” *Scientific Reports* **9**, 19462 (2019).
- 1081 ³⁶Y. J. Gu and S. V. Bulanov, “Magnetic field annihilation and charged particle acceleration in
1082 ultra-relativistic laser plasmas,” *High Power Laser Science and Engineering* **9**, E2 (2021).
- 1083 ³⁷B. N. Kuvshinov, E. Westerhof, T. J. Schep, and M. Berning, “Electron magnetohydrodynamics
1084 of magnetized inhomogeneous plasmas,” *Phys. Lett. A* **241**, 287 (1998).
- 1085 ³⁸N. Attico, F. Califano, and F. Pegoraro, “Charge separation effects in electron-
1086 magnetohydrodynamic reconnection,” *Phys. Plasmas* **16**, 2381–2387 (2000).
- 1087 ³⁹D. Del Sarto, F. Califano, and F. Pegoraro, “Current layer cascade in collisionless electron
1088 magnetohydrodynamic reconnection and electron compressibility effects,” *Phys. Plasmas* **12**,
1089 012317 (2005).
- 1090 ⁴⁰D. Del Sarto, F. Califano, and F. Pegoraro, “Electron parallel compressibility in the nonlinear
1091 development of two-dimensional magnetohydrodynamic reconnection,” *Mod. Phys. Lett. B* **20**,
1092 931–961 (2006).
- 1093 ⁴¹Biermann, L., and (mit einem Anhang von A. Schütler), “Über den Ursprung der Magnetfelder
1094 auf Sternen und im interstellaren Raum,” *Zeitschrift Naturforschung Teil A* **5**, 65 (1950).
- 1095 ⁴²T. M. Abdalla, B. N. Kuvshinov, T. J. Schep, and E. Westerhof, “Electron vortex generation by
1096 strong, localized plasma heating,” *Phys. Plasmas* **8**, 3957 (2001).
- 1097 ⁴³A. V. Gordeev and L. I. Rudakov, “Instability of a plasma in a strongly inhomogeneous mag-
1098 netic field,” *Zh. Exsp. Teor. Fiz.* **55**, 2310 (1958).
- 1099 ⁴⁴D. Y. Yoon and P. M. Bellan, “The electron canonical battery effect in magnetic reconnection:
1100 completion of the electron canonical vorticity framework,” *Phys. Plasmas* **26**, 100702 (2019).
- 1101 ⁴⁵T. S. Wood, R. Hollerbach, and M. Lyutikov, “Density-shear instability in electron magneto-
1102 hydrodynamics,” *Phys. Plasmas* **21**, 052110 (2014).
- 1103 ⁴⁶M. Lyutikov, “Magnetar activity mediated by plastic deformations of neutron star crust,”
1104 *Monthly Not. Royal Astr. Soc.* **447**, 1407–1417 (2015).
- 1105 ⁴⁷H. Cai and D. Li, “Magnetic reconnection with pressure gradient in compressible electron mag-
1106 netohydrodynamics,” *Phys. Plasmas* **15**, 042101 (2008).
- 1107 ⁴⁸H. Cai and D. Li, “Magnetic reconnection with pressure tensor in electron magnetohydrody-
1108 namics,” *Phys. Plasmas* **16**, 052107 (2009).

- ⁴⁹H. Cai and D. Li, “Tearing modes in electron-magnetohydrodynamic instabilities,” in *Proceedings of the 23rd IAEA Fusion Energy Conference, IAEA-CN-180* (IAEA Publications, 2010) pp. THS/P5–03.
- ⁵⁰B. Basu, “Moment equation description of weibel instability,” *Phys. Plasmas* **9**, 5131 (2002).
- ⁵¹Sarrat, M. and Del Sarto, D. and Ghizzo, A., “ Fluid description of Weibel-type instabilities via full-pressure tensor dynamics ,” *EuroPhys. Lett.* **115**, 45001 (2016).
- ⁵²Sarrat, M. and Del Sarto, D. and Ghizzo, A., “ A pressure tensor description for the time-resonant Weibel instability ,” *J. Plasma Phys.* **83**, 705830103 (2017).
- ⁵³P. M. A. Dirac, “A new classical theory of electrons. ii,” *Proc. R. Soc. London Ser. A* **212**, 330 (1952).
- ⁵⁴J. A. Schouten, *Tensor analysis for physicists (Second edition)* (Dover Publications, New York, 1989).
- ⁵⁵H. Alfvén, “Existence of electromagnetic-hydrodynamics waves,” *Nature* **150**, 405 (1942).
- ⁵⁶L. Woltjer, “A theorem on force-free magnetic fields,” *Proc. Natl. Acad. Sci. USA* **44**, 489 (1958).
- ⁵⁷W. A. Ncomb, “Motion of magnetic lines of force,” *Annals of Physics* **3**, 347 (1958).
- ⁵⁸S. Kingsep, K. V. Chukbar, and V. V. Yan’kov, “Electron magnetohydrodynamics,” **16** (1990).
- ⁵⁹A. V. Gordeev and L. I. Kingsep, A. S. and Rudakov, “Electron magnetohydrodynamics,” *Physics Reports* **243**, 215–315 (1994).
- ⁶⁰J. P. Klozenberg, B. McNamara, and P. C. Thonemann, “The dispersion and attenuation of helicon waves in a uniform cylindrical plasma,” *J. Fluid. Mech.* **21**, 545 (1965).
- ⁶¹A. A. Chernov and V. V. Yan’kov, “Electron fluxes in low density pinches,” *Fizika Plazmy* **8**, 931 (1982).
- ⁶²M. B. Isichenko and A. M. Marnachev, “Nonlinear structures in the electron magnetohydrodynamics of a homogeneous plasma,” *Sov. Phys. JETP* **66**, 702 (1987).
- ⁶³I. A. Ivonin, “Stability of 2d vortices against 3d perturbations in a fluid in electro hydrodynamics,” *Sov. J. Plasma Phys.* **18**, 302 (1992).
- ⁶⁴L. Uby, M. B. Isichenko, and V. V. Yankov, “Vortex filament dynamics in plasmas and superconductors,” *Phys. Rev. E* **52**, 932 (1995).
- ⁶⁵S. V. Bulanov, M. Lontano, T. Esirkepov, P. F., and A. M. Pukhov, “Electron vortices produced by ultraintense laser pulses,” *Phys. Rev. Lett.* **76**, 3652 (1996).

- ⁶⁶A. Das, “Nonlinear aspects of two-dimensional electron magnetohydrodynamics,” *Plasma Phys. Controll. Fusion* **41**, A531 (1999).
- ⁶⁷D. Jovanovich and F. Pegoraro, “Two-dimensional electron-magnetohydrodynamic nonlinear structures,” *Phys. Plasmas* **7**, 889 (2000).
- ⁶⁸B. N. Kuvshinov, J. Rem, T. J. Schep, and E. Westerhof, “Electron vortices in magnetized plasmas,” *Phys. Plasmas* **8**, 3232 (2001).
- ⁶⁹P. Shukla and L. Stenflo, “Comment on “Electron vortices in magnetized plasmas”[*Phys. Plasmas* **8**, 3232 (2001)],” *Phys. Plasmas* **8**, 5061–5062 (2001).
- ⁷⁰S. Dastgeer, “Generation of coherent structures in electron magnetohydrodynamics,” *Phys. Scripta* **69**, 216 (2004).
- ⁷¹R. Stenzel, J. Urrutia, and M. Griskey, “On conservation of helicity and energy of reflecting electron magnetohydrodynamic vortices,” *Phys. Review L. Lett.* **82**, 4006 (1999).
- ⁷²J. M. Urrutia, R. L. Stenzel, and M. C. Griskey, “Laboratory studies of magnetic vortices. iii. collisions of electron magnetohydrodynamic vortices,” *Phys. Plasmas* **7**, 519 (2000).
- ⁷³R. L. Stenzel, J. M. Urrutia, and C. L. Rousculp, “Helicities of electron magnetohydrodynamic currents and filaments,” *Phys. Rev. Lett.* **74**, 702 (1995).
- ⁷⁴R. L. Stenzel and J. M. Urrutia, “Helicity and transport in electron mhd,” *Phys. Rev. Lett.* **76**, 1469 (1995).
- ⁷⁵C. L. Rousculp and Stenzel, “Helicity injection by knotted antennas into electron magnetohydrodynamical plasmas,” *Phys. Rev. Lett.* **79**, 837 (1997).
- ⁷⁶R. L. Stenzel, J. M. Urrutia, and K. Strohmaier, “Whistler modes with wave magnetic fields exceeding the ambient magnetic field,” *Phys. Rev. Lett.* **96**, 095004 (2006).
- ⁷⁷R. L. Stenzel and J. M. Urrutia, “Helicons in unbounded plasmas,” *Phys. Rev. Lett.* **114**, 205005 (2015).
- ⁷⁸D. Biskamp, E. Schwarz, and J. F. Drake, “Two-dimensional electron magnetohydrodynamic turbulence,” *Phys. Rev. Lett.* **76**, 1264 (1996).
- ⁷⁹D. Biskamp, E. Schwarz, and A. Celani, “Nonlocal bottleneck effect in two-dimensional turbulence,” *Phys. Rev. Lett.* **81**, 4855 (1998).
- ⁸⁰D. Biskamp, E. Schwarz, A. Zeiler, A. Celani, and J. F. Drake, “Electron magnetohydrodynamic turbulence,” *Phys. Plasmas* **6**, 751 (1999).
- ⁸¹A. Celani, R. Prandi, and G. Boffetta, “Kolmogorob’s law for two-dimensional electron-magnetohydrodynamic turbulence,” *EuroPhys. Lett.* **41**, 13 (1998).

- ⁸²G. Boffetta, A. Celanin, A. Crisanti, and A. Prandi, “Intermittency of two-dimensional decaying electron magnetohydrodynamic turbulence,” *Phys. Rev. E* **59**, 3724 (1999).
- ⁸³T. M. Abdalla, V. P. Lakhin, T. J. Schep, and E. Westerhof, “Spectral properties of decaying turbulence in electron magnetohydrodynamics,” *Phys. Plasmas* **10**, 3007 (2003).
- ⁸⁴V. P. Lakhin and T. J. Schep, “On the generation of mean fields by small-scale electron magnetohydrodynamic turbulence,” *Phys. Plasmas* **11**, 1424 (2004).
- ⁸⁵M. Kono and H. L. Pécseli, “Cascade conditions in electron magnetohydrodynamic turbulence,” *Phys. Plasmas* **29**, 122305 (2022).
- ⁸⁶A. Das and P. Kaw, “Nonlocal suassage like instability of current chammels in electron magnetohydrodynamics,” *Phys. Plasmas* **8**, 4518 (2001).
- ⁸⁷G. Gaur, S. Sundar, S. K. Yadav, A. Das, P. Kaw, and S. Sharma, “Role of natural length and time scales on shear driven two-dimensional electron magnetohydrodynamic instability,” *Phys. Plasmas* **16**, 072310 (2009).
- ⁸⁸A. Gaur, G. and Das, “Linear and nonlinear studies of velocity shear driven three dimensional electron-magnetohydrodynamics instability,” *Phys. Plasmas* **19**, 072103 (2012).
- ⁸⁹F. Califano, R. Prandi, F. Pegoraro, and B. S. V., “Two-dimensional electron-magnetohydrodynamic instabilities,” *Phys. Plasmas* **6**, 2332 (1999).
- ⁹⁰H. Cai and D. Li, “Tearing mode with guide field gradient in electron magnetohydrodynamics,” *Phys. Plasmas* **16**, 022109 (2009).
- ⁹¹D. Del Sarto, F. Califano, and F. Pegoraro, “Secondary instabilities and vortex formation in collisionless-fluid magnetic reconnection,” *Phys. Rev. Lett.* **91**, 235001 (2003).
- ⁹²L. Chacón, A. N. Simakov, and A. Zocco, “Steady-state properties of driven magnetic reconnection in 2d electron magnetohydrodynamics,” *Phys. Review Lett.* **99**, 235001 (2007).
- ⁹³N. Jain and A. S. Sharma, “Evolution of electron current sheets in collisionless magnetic reconnection,” *Phys. Plasmas* **22**, 102110 (2015).
- ⁹⁴D. Y. Yoon and P. M. Bellan, “A generalized two-fluid picture of non-driven collisionless reconnection and its relation to whistler waves,” *Phys. Plasmas* **24**, 052114 (2017).
- ⁹⁵D. Y. Yoon and P. M. Bellan, “An intuitive two-fluid picture of spontaneous 2d collisionless reconnection and whistler wave generation,” *Phys. Plasmas* **25**, 055704 (2018).
- ⁹⁶J. C. Dorelli and J. Birn, “Electron magnetohydrodynamic simulations of magnetic island coalescence,” *Phys. Plasmas* **8**, 4010 (2001).

- ⁹⁷V. P. Zhukov, “Coalescence instability in the electron magnetohydrodynamics,” *Plasma Phys. Rep.* **28**, 411 (2002).
- ⁹⁸A. Tenerani, F. A. Rappazzo, M. Velli, and F. Pucci, “The tearing mode instability in thin current sheets: the transition to fast reconnection in the presence of viscosity,” *Astrophys. J.* **801**, 145 (2015).
- ⁹⁹Bian, N. H. and Tsiklauri, D., “Compressible hall magnetohydrodynamics in a strong magnetic field,” *Phys. Plasmas* **16**, 064503 (2009).
- ¹⁰⁰J. F. Drake, R. G. Kleva, and M. E. Mandt, “Structure of thin current layers: implications for magnetic reconnection,” *Phys. Rev. Lett.* **73**, 1251 (1994).
- ¹⁰¹M. E. Mandt, R. E. Denton, and J. F. Drake, “Transition to whistler mediated magnetic reconnection,” *J. Geophys. Res.* **21**, 73 (1994).
- ¹⁰²D. Biskamp, E. Schwarz, and J. F. Drake, “Two-fluid theory of collisionless magnetic reconnection,” *Phys. Plasmas* **4**, 1002 (1997).
- ¹⁰³Birn, J. and Drake, J. F. and Shay, M. A. and Rogers, B. N. and Denton, R. E. and Hesse, M. and Kutzsentsova, M. and Ma, Z. W. and Bhattacharjee, A. and Otto, A. and Pritchett, P. L., “Geospace Environmental Modeling (GEM) Magnetic Reconnection Challenge,” *J. Geophys. Res.* **106**, 3715 (2001).
- ¹⁰⁴B. N. Rogers, R. E. Denton, J. F. Drake, and M. A. Shay, “Role of dispersive waves in collisionless magnetic reconnection,” *Phys. Rev. Lett.* **87**, 195004 (2001).
- ¹⁰⁵M. A. Shay, J. F. Drake, and B. N. Rogers, “Alfvénic collisionless reconnection and the hall term,” *J. Geophys. Res.* **106**, 3759 (2001).
- ¹⁰⁶Singh, N. and Deverapalli, C. and Khazanov, G., “Electrodynamics in a very thin current sheet leading to magnetic reconnection,” *Nonlin. Proc. Geophys.* **13**, 509–523 (2006).
- ¹⁰⁷Bian, N. H. and Vekstein, G., “On the two-fluid modification of the resistive tearing instability,” *Phys. Plasmas* **14**, 072107 (2007).
- ¹⁰⁸J. F. Drake, M. A. Shay, and M. Swisdak, “The hall fields and fast magnetic reconnection,” *Phys. Plasmas* **15**, 042306 (2008).
- ¹⁰⁹P. Bellan, “Fast, purely growing collisionless reconnection as an eigenfunction problem related to but not involving linear whistler waves,” *Phys. Fluids* **21**, 102108 (2014).
- ¹¹⁰F. Pucci, M. Velli, and A. Tenerani, “Fast magnetic reconnection: “ideal” tearing and the Hall effect,” *Astrophys. J.* **845**, 25 (2017).

- ¹¹¹G. Vekstein, “On the hall-mediated resistive tearing instability of highly elongated current sheets,” *Phys. Plasmas* **26**, 012106 (2019).
- ¹¹²F. Pucci and M. Velli, “Reconnection of quasi-singular current sheets: the "ideal" tearing mode,” *Astrophys. J. Lett.* **780**, L19 (2014).
- ¹¹³N. Jain and A. S. Sharma, “Electron-scale nested quadrupole Hall field in Cluster observations of magnetic reconnection,” in *Annales Geophysicae*, Vol. 33 (2015) pp. 719–724.
- ¹¹⁴L. Franci, E. Papini, A. Micera, G. Lapenta, P. Hellinger, D. Del Sarto, D. Burgess, and S. Landi, “Anisotropic electron heating in turbulence-driven magnetic reconnection in the near-sun solar wind,” *Astrophys. J.* **936**, 27 (2022).
- ¹¹⁵H.-J. Cai and L. C. Lee, “The generalized ohm’s law in collisionless magnetic reconnection,” *Phys. Plasmas* **4**, 509–520 (1997).
- ¹¹⁶M. Dobrowolny, “Kelvin-helmholtz instability in a high- β collisionless plasma,” *Phys. Fluids* **15**, 2263–2270 (1972).
- ¹¹⁷I. Hofman, “Resistive tearing modes in a sheet pinch with shear flow,” *Plasma Phys.* **17**, 143 (1975).
- ¹¹⁸G. Einaudi and F. Rubini, “Resistive instabilities in a flowing plasma: I. Inviscid case,” *Phys. Fluids* **29**, 2563–2568 (1986).
- ¹¹⁹X. Chen and P. Morrison, “Resistive tearing instability with equilibrium shear flow,” *Physics of Fluids B: Plasma Physics* **2**, 495–507 (1990).
- ¹²⁰D. Borgogno, D. Grasso, B. Achilli, M. Romé, and L. Comisso, “Coexistence of plasmoid and Kelvin–Helmholtz instabilities in collisionless plasma turbulence,” *Astrophys. J.* **929**, 62 (2022).
- ¹²¹S. V. Bulanov, J. Sakai, and S. I. Syrovatskii, “Tearing-mode instability in approximately steady mhd configurations,” *Fizika Plazmy* **5**, 280–290 (1979).
- ¹²²S. Syrovatskii, “Pinch sheets and reconnection in astrophysics,” *Annual Rev. Astron. and Astrophys.* **19**, 163–227 (1981).
- ¹²³K.-I. Nishikawa, “Stabilizing effect of a normal magnetic field on the collisional tearing mode,” *Phys. Fluids* **25**, 1384 (1982).
- ¹²⁴B. V. Somov and A. I. Verneta, “Magnetic reconnection in a high-temperature plasma of solar flares. iii. stabilizing effect of the transverse magnetic field in a non-neutral current sheet,” *Solar Phys.* **117**, 89 (1988).

- ¹²⁵E. Papini, L. Franci, S. Landi, A. Verdini, L. Matteini, and P. Hellinger, “Can hall magnetohydrodynamics explain plasma turbulence at sub-ion scales?” *Astrophys. J.* **870**, 52 (2019).
- ¹²⁶G. Bertin, “Effects of local current gradients on magnetic reconnection,” *Phys. Rev. A* **25**, 1786 (1982).
- ¹²⁷F. Militello, G. Huysmans, M. Ottaviani, and F. Porcelli, “Effects of local features of the equilibrium current density profile on linear tearing modes,” *Phys Plasmas* **11**, 125–128 (2004).
- ¹²⁸M. Dubois and A. Samain, “Asymmetrical tearing mode in a collisional plasma,” *Plasma Phys.* **21**, 101 (1979).
- ¹²⁹J. Killeen and A. Shestakov, “Effect of equilibrium flow on the resistive tearing mode,” *Phys. Fluids* **21**, 1746–1752 (1978).
- ¹³⁰G. Einaudi and F. Rubini, “Effects of asymmetry on collisional tearing mode,” *Nuovo Cimento B* **81**, 102–110 (1984).
- ¹³¹F. Militello, D. Borgogno, D. Grasso, C. Marchetto, and M. Ottaviani, “Asymmetric tearing mode in the presence of viscosity,” *Phys. Plasmas* **18**, 112108 (2011).
- ¹³²F. Ebrahimi, “Dynamo-driven plasmoid formation from a current-sheet instability,” *Phys. Plasmas* **23**, 120705 (2016).
- ¹³³H.-W. Xu, H.-W. Zhang, Y.-H. Song, Z.-W. Ma, and Y.-N. Wang, “Simulation studies of the radiation-driven tearing mode in tokamaks,” *Plasma Phys. Controll. Fusion* **62**, 105009 (2020).
- ¹³⁴W. Guo, D. Liu, X. Wang, and J. Wang, “Tearing mode analysis in electron magnetohydrodynamics with pressure gradient,” *AIP Advances* **10**, 105207 (2020).
- ¹³⁵S. Boldyrev and N. F. Loureiro, “Role of reconnection in inertial kinetic-alfvén turbulence,” *Physical Rev. Res.* **1**, 012006 (2019).
- ¹³⁶C. H. K. Chen and S. Boldyrev, “Nature of kinetic scale turbulence in the earth’s magnetosheath,” *Astrophys. J.* **842**, 122 (2017).
- ¹³⁷F. Porcelli, D. Borgogno, F. Califano, D. Grasso, M. Ottaviani, and F. Pegoraro, “Recent advances in collisionless magnetic reconnection,” *Plasma Phys. Controll. Fusion* **44**, B389 (2002).
- ¹³⁸M. Ottaviani and F. Porcelli, “Fast nonlinear magnetic reconnection,” *Phys. Plasmas* **2**, 4104–4117 (1995).
- ¹³⁹F. Pegoraro and T. J. Schep, “Theory of resistive modes in the ballooning representation,” *Plasma Phys. Controll. Fusion* **28**, 647 (1986).
- ¹⁴⁰C. Granier, D. Borgogno, D. Grasso, and E. Tassi, “Gyrofluid analysis of electron β_e effects on collisionless reconnection,” *J. Plasma Phys.* **88**, 905880111 (2022).

- ¹²⁹⁷ ¹⁴¹S. I. Braginskii, “Transport processes in a plasma,” *Reviews of Plasma Physics* **1**, 205 (1965).
- ¹²⁹⁸ ¹⁴²J. D. Huba, *NRL Plasma Formulary* (Naval Research Laboratory, Washington, DC, 2007 (re-
- ¹²⁹⁹ revised)).
- ¹³⁰⁰ ¹⁴³S. J. L., “Equations of motion for an ideal plasma.” *The Astrophysical Journal* **116**, 299 (1952).
- ¹³⁰¹ ¹⁴⁴J. L. Spitzer and R. Härm, “Transport phenomena in a completely ionized gas,” *Physical Review*
- ¹³⁰² **89**, 977 (1953).
- ¹³⁰³ ¹⁴⁵A. Kuritsyn, M. Yamada, S. Gerhardt, H. Ji, R. Kulsrud, and Y. Ren, “Measurements of the par-
- ¹³⁰⁴ allel and transverse spitzer resistivities during collisional magnetic reconnection,” *Phys. Plas-*
- ¹³⁰⁵ *mas* **13**, 055703 (2006).
- ¹³⁰⁶ ¹⁴⁶M. Moncuquet, N. Meyer-Vernet, K. Issautier, M. Pulupa, J. W. Bonnell, S. D. Bale, T. D.
- ¹³⁰⁷ de Wit, K. Goetz, L. Griton, P. R. Harvey, R. J. MacDowall, M. Maksimovic, and D. M.
- ¹³⁰⁸ Malaspina, “First in situ measurements of electron density and temperature from quasi-thermal
- ¹³⁰⁹ noise spectroscopy with Parker solar probe/Fields,” *Astrophys. J. Suppl. Series* **246**, 44 (2020).
- ¹³¹⁰ ¹⁴⁷D’Amicis, R. and Perrone, D. and Bruno, R. and Velli, M., “On Alfvénic slow wind: a journey
- ¹³¹¹ from the Earth back to the Sun,” *J. Geophys. Res. —Space Phys.* **126**, e2020JA028996 (2021).
- ¹³¹² ¹⁴⁸J. V. Hollweg, “Viscosity and the Chew-Goldberger-Low equations in the solar corona,” *Astro-*
- ¹³¹³ *physical Journal, Part 1* (ISSN 0004-637X), vol. 306, July 15, 1986, p. 730-739. **306**, 730–739
- ¹³¹⁴ (1986).
- ¹³¹⁵ ¹⁴⁹P. Holoborodko, “Advanpix multiprecision computing tool for MATLAB,” (2012).